N° Ordre ..... /FHC/UMBB/2023

REPUBLIQUE ALGERIENNE DEMOCRATIQUE ET POPULAIRE
MINISTERE DE L'ENSEIGNEMENT SUPERIEUR ET DE LA RECHERCHE SCIENTIFIQUE
UNIVERSITE M'HAMED BOUGARA-BOUMERDES

Faculté des Hydrocarbures et de la Chimie
Mémoire de Fin d'Etudes
En vue de l'obtention du diplôme :

MASTER

Présenté par :

MOKHTACHE ISLEM

HEDNA ABDERRAHMEN

Filière : Hydrocarbures
Spécialité : Automatisation des procédés industriels : Commande Automatique

Thème

Evolving intelligent control of three-phase separator level loop with slug flow compensation

---

Devant le jury :

KESRAOUI M.	Prof.	UMBB	Président
CHAIB A.	Prof.	UMBB	Examinateur
HABBI H.	Prof.	UMBB	Encadreur

Année universitaire 2022/2023

N° Ordre ..... /FHC/UMBB/2023

REPUBLIQUE ALGERIENNE DEMOCRATIQUE ET POPULAIRE
MINISTERE DE L'ENSEIGNEMENT SUPERIEUR ET DE LA RECHERCHE SCIENTIFIQUE
UNIVERSITE M'HAMED BOUGARA-BOUMERDES

Faculté des Hydrocarbures et de la Chimie
Département : Automatisation et Electrification des procédés
Filière : Hydrocarbures

Spécialité : Automatisation des procédés industriels : Commande Automatique

Mémoire de Fin d'Etudes
En vue de l'obtention du diplôme :

MASTER

Thème

Evolving intelligent control of three-phase separator level loop with slug flow compensation

---

Présenté par :
MOKHTACHE ISLEM
HEDNA ABDERRAHMEN

Avis favorable de l'encadreur :
Pr. HABBI HACENE **Signature**

Avis favorable du Président du jury
Nom Prénom **Signature**

Cachet et signature

Acknowledgments

First and foremost, we thank God, ALLAH, the Almighty and Merciful, for giving us the strength and patience to successfully complete this modest work.

We would like to express our deep appreciation to our scientific supervisor, Mr. HABBI Hacene, for overseeing this work and for the continuous encouragement he has provided us. We are grateful to be able to extend our sincerest thanks to him.

We thank all the members of the jury who agreed to examine this manuscript. Our heartfelt thanks to all our teachers who have accompanied us throughout our academic journey at the Faculty of Hydrocarbons and Chemistry (formerly known as INH) at M'Hamed Bougara University.

We cannot conclude without expressing our gratitude to our kind parents, brothers, and sisters for their support during these years.

We would like to express our sincere gratitude to the engineer Mr.ZIKARA.K who provided invaluable assistance and support during the course of our internship. Their expertise and guidance have been instrumental in the successful completion of our project.

We would like to express our gratitude to our friends and classmates who have provided support and encouragement along the way. Their companionship and shared experiences have made this journey more enjoyable.

To everyone who has contributed in any way, big or small, I offer my heartfelt thanks. Your support has been instrumental in the successful completion of this project.

Dedications

To our parents, who have cared for our education and well-being, we will never find enough words to express our love and gratitude. Your unwavering support and sacrifices have shaped us into the individuals we are today. Thank you for believing in us and for always being there.

To our dear brothers and sisters, you hold a special place in our hearts. We appreciate your presence and the bond we share.

To our MOKHTACHE and HEDNA families, thank you for being a part of our lives. Your love and support have meant the world to us.

To our friends, you have been there for us when we needed a shoulder to lean on. We are grateful for your friendship and unwavering support.

To all those who are dear to us and have supported us, we extend our heartfelt thanks. You have stood by us in our times of need, and we cherish your presence in our lives.

Contents

List of Figures

List of Tables

Symbols and notations

r	Radius of the separator [m]
D	Diameter of the separator [m]
h_w	Height of the weir [m]
L	Length of the separator [m]
l_w	Length of the water compartment [m]
A	Oil surface in separator [m^2]
m_w	Mass of water [kg]
m_g	Mass of the gas [kg]
G	Acceleration of gravity [m/s^2]
H	Separator liquid level [m]
M	Molar gas constant [Mol]
P	Separator pressure [Pa]
R	Gas constant $[\frac{j}{k.Mol}]$
T	Separator temperature [K]
q_{iw}, q_{ow}	Inlet, outlet water volume flow [m^3/s]
q_{io} , q_{oo}	Inlet, outlet oil volume flow [m^3/s]
w_{ig} , w_{ig}	Inlet, outlet mass flow rate of gas [kg/s]
V_w	Volume of water [m^3]
V_o	Volume of oil [m^3]
V_g	Volume of gas [m^3]
ρ_w	Water density [kg/m^3]
ρ_o	Oil density [kg/m^3]
ρ_g	Gas density [kg/m^3]
Ω	Frequency [rad/s]
ω_c	Crossover frequency [rad/s]

ω_t	Closed loop frequency at -3dB [rad/s]
ω_{180}	Phase crossing frequency [rad/s]
T	Time constant [s]
K_{cr}	Critical gain
T_{cr}	Period of oscillations
k_p	Proportional gain
T_i	Integration constant
T_d	Differentiation constant
$R(s)$	Transfer function of the PID
θ	Time delay associated with the process
w_0	Resonant frequency
Ç	Damping factor
r_I	Integration time constant
e_k	Control error
s_k	Tracking error
y_k^r	Reference model output
γ_k^i	Local density
μ_k^i	Mean value
σ_k^i	Mean-squared length

Introduction

The performance and operational efficiency of petroleum processes are of utmost importance in the oil and gas industry. Water-oil-gas separators are critical components of oil production facilities in view of the crucial role they play in the separation of oil, water and gas. More specifically, it is of substantial interest to keep high operational performance of the separator through proper controlling of the main control loops which are the water level loop, the oil level loop and the gas pressure loop. Level control is often challenging since most of emergency shutdowns in industrial separators are caused by poor level control, which might be caused by high loads, flow slugging, process dynamics changes, controllers detuning, among many other reasons.

Conventional control methods which are basically model-based approaches have shown several limitations in dealing with the nonlinear dynamics of the physical separator. This project focuses on the problem of level control in a three-phase separator. We studied on a simulated model of the industrial separator 10-V-255 which is part of the oil and gas production unit located in a centre called GS1, which is a collection field for oil production from an entire site grouping GS-1, ARs, and ZOTTI. The separator process ensures efficient separation of the different phases, allowing for the production of high-quality oil and gas products that meet the required specifications. However, the effective control of the main control loops imposes significant challenges due to the dynamic nature of the process and the inherent complexities involved.

Throughout this study, we fundamentally aim to improve the existing control structure by using a model-free control method, namely the Robust Evolving Cloud-based Control (RECCo) strategy which is a fully unsupervised controller that learns the control structure and parameters concurrently from data streams without any prior modeling of the controlled plant. The suggested intelligent evolving control system is compared to other classical and advanced control methods to verify its effectiveness. Compared methods include distinct tuning approaches of PID

controllers, namely particle swarm optimization (PSO) based tuning method, Ziegler-Nichols (ZN) PID tuning method and Skogestad's Internal Model Control (SIMC) method.

In this study, we first develop a mathematical model of the 10-V-255 separator relying on first-principle laws. Models describing the water level dynamics, the oil level dynamics and gas pressure dynamics are derived based on physical equations. These models are used for process dynamics analysis and PID controllers tuning. It is worth noting that the design method of the RECCo controller does not require any process modeling; the constructed water level model is employed here for the sake of simulation only.

Simulations are performed under different scenarios to assess the effectiveness of the RECCo controller in regulating the water level of the 10-V-255 three-phase separator and compensating for the slugging effect. To this end, we use various performance metrics, including control accuracy, stability, response time, and robustness to disturbances. The comparison with the PID-ZN, the PID-PSO and the PID-SIMC controllers aims to provide insights into the advantages and limitations of the self-evolving RECCo controller in this specific case study.

The findings of this study are expected to contribute to the advancement of control strategies for three-phase separators in the oil and gas industry. By harnessing the capabilities of the RECCo controller, we aim to enhance the overall efficiency, safety, and productivity of the 10-V-255 separator, ultimately leading to optimized oil and gas production processes.

This manuscript is organized in three chapters. The first chapter introduces the oil production separator processes with detailed description of industrial control structures involved. The second chapter describes the modeling phase of the 10-V-255 separator and presents the derived mathematical models for water level, oil level and gas pressure. Control structure design and tuning is presented in the third chapter, where the design methods of the RECCo controller, the PID-ZN controller, the PID-PSO controller and the PID-SIMC controller are detailed. This chapter also summarizes the control results and compares the considered controllers under level reference tracking and slugging effect compensation scenarios.

CHAPTER I Multi-phase separators in oil and gas production facilities

I.1 Introduction

In the petroleum industry, the extraction of crude oil often involves the production of not only oil but also associated gas and water. The three-phase separation process is designed to separate these three components efficiently, enabling the isolation of valuable oil and gas while treating the produced water for proper disposal or reutilization. This procedure employs specialized equipment and methods to achieve effective separation and plays a critical role in maximizing production efficiency and ensuring compliance with environmental regulations.

The three-phase separation process typically takes place in a facility called a separator. This separator may be a vertical or horizontal vessel that utilizes gravity and specific internal components to facilitate the separation of oil, water, and gas. The separation relies on the differences in density, viscosity, and volatility of the three phases.

I.2 Multi-phase separation process

I.2.1 Inlet zone

In this step, the well stream enters the separator through an inlet device that reduces its velocity and distributes it evenly [1]. The inlet device can be a simple pipe tee, a half-open pipe, a deflector plate, or a cyclone [2]. The inlet device also helps to remove large liquid slugs and solid particles from the well stream. For example, a cyclone inlet device can separate up to 80% of the liquid from the gas by centrifugal force [3].

I.2.2 Flow distribution zone

In this step, baffles are used to prevent turbulence and enhance separation [1]. The baffles can be perforated plates, wire mesh pads, or vane packs [2]. They also help to coalesce small liquid droplets into larger ones. For example, a vane pack baffle can increase the droplet size by 10 times by forcing the gas to flow through parallel plates with small gaps [4].

I.2.3 Gravity/coalescing zone

In this step, the gas and liquid phases separate by gravity, while coalescing devices help to remove small droplets from each phase [1]. The coalescing devices can be plate coalescers, cyclone tubes, or electrostatic grids [2]. They increase the efficiency of separation by increasing the residence time and reducing the droplet size distribution. For example, an electrostatic grid coalescer can apply an electric field to charge and attract the droplets to each other and to the electrodes [5].

I.2.4 Outlet zone

In this step, mist extractors remove any remaining liquid from the gas phase, while weirs and level controllers regulate the liquid level and interface [1]. The mist extractors can be wire mesh pads, vane packs, cyclone tubes, or fiber beds [2]. They capture small liquid droplets and solid particles from the gas stream before it leaves the separator. For example, a wire mesh pad mist extractor can trap up to 99% of the droplets larger than 10 microns by impingement and coalescence [6].

The weirs and level controllers control the liquid level or interface level by adjusting the flow rate of each liquid phase through a level valve. Vortex breakers prevent gas entrainment in the liquid phase by disrupting the swirling motion of the liquid at the outlet nozzle [1]. The outlet zone is critical for ensuring the quality of the separated phases and avoiding carryover or carryunder problems [2].

The separated gas and liquid phases exit the separator through their respective outlets, where pressure controllers and valves maintain the desired pressure in the separator [1].

I.3 Industrial separators

Generally there are two types of separators: two-phase separators which are used for separating crude oil and gas, and three-phase separators that can separate oil, gas and water.

I.3.1 The definition of a separator

Petroleum separators are devices that separate the gaseous and liquid components of a well stream into different phases. They are essential for oil and gas processing, as they allow for the measurement, storage, and transportation of each phase. Petroleum separators can have different configurations, such as horizontal, vertical, or spherical, depending on the flow

conditions and design requirements. They can also operate in two-phase or three-phase mode, depending on whether water is present in the well stream or not [1]. Accordingly, there are two types of separators: two-phase separators which are used for separating crude oil and gas, and three-phase separators that can separate oil, gas and water.

I.3.2 Separator types

There are various types of separators used in different industries for the separation of fluids or gases based on their properties. Below are given some common types of separators.

I.3.2.1 Vertical Separator

A vertical separator (Fig. I.1) is a type of separator where the separation of fluids or gases occurs vertically. It is commonly used in industries such as oil and gas, where it is employed to separate oil, gas, and water. The fluids or gases enter the separator from the top and separate based on their density, with the lighter components rising to the top and the heavier components settling at the bottom.

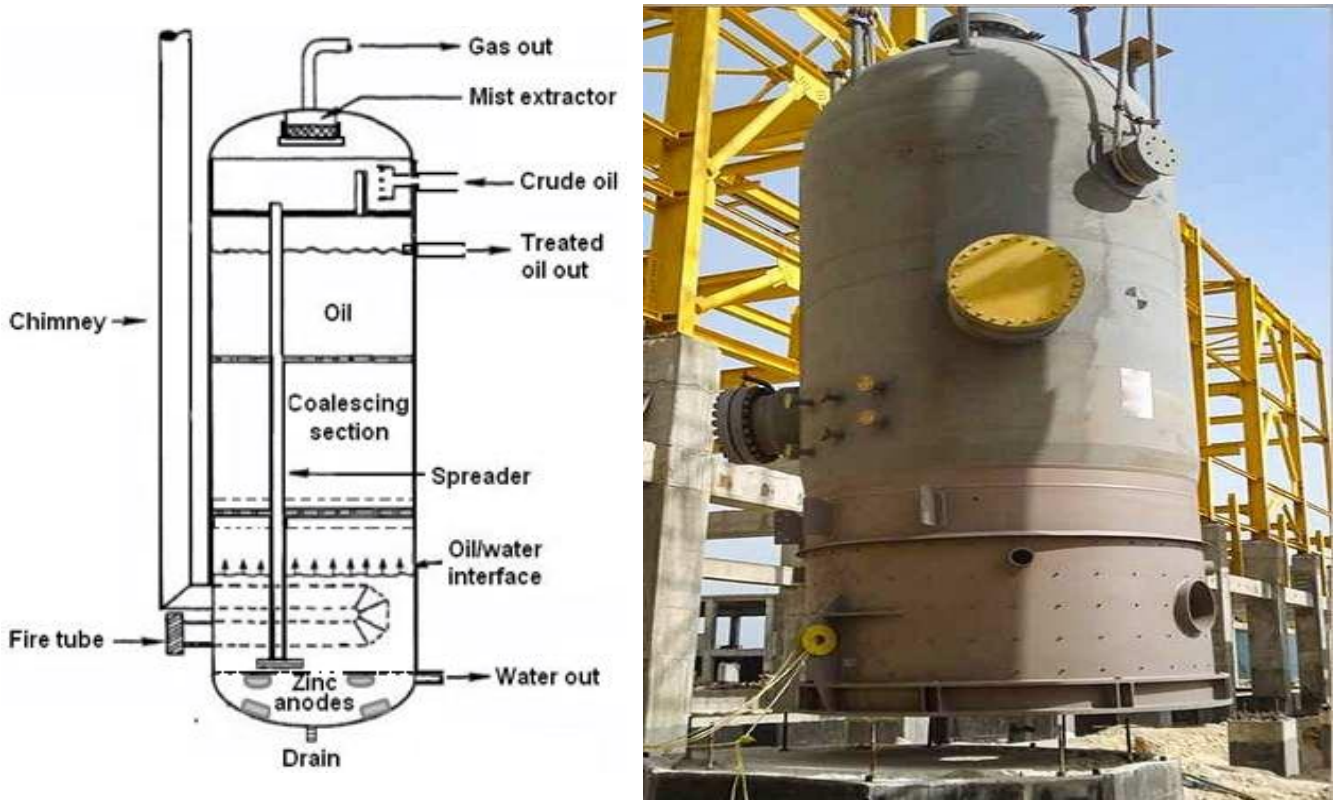

Figure I.1 Vertical separator [2]

I.3.2.2 Horizontal Separator

An horizontal separator (Fig. I.2) is a separator where the separation process occurs horizontally. It is also commonly used in oil and gas industries for the separation of oil, gas, and water. The fluids or gases enter the separator from the side and separate based on their density, with the lighter components accumulating at the top and the heavier components collecting at the bottom.

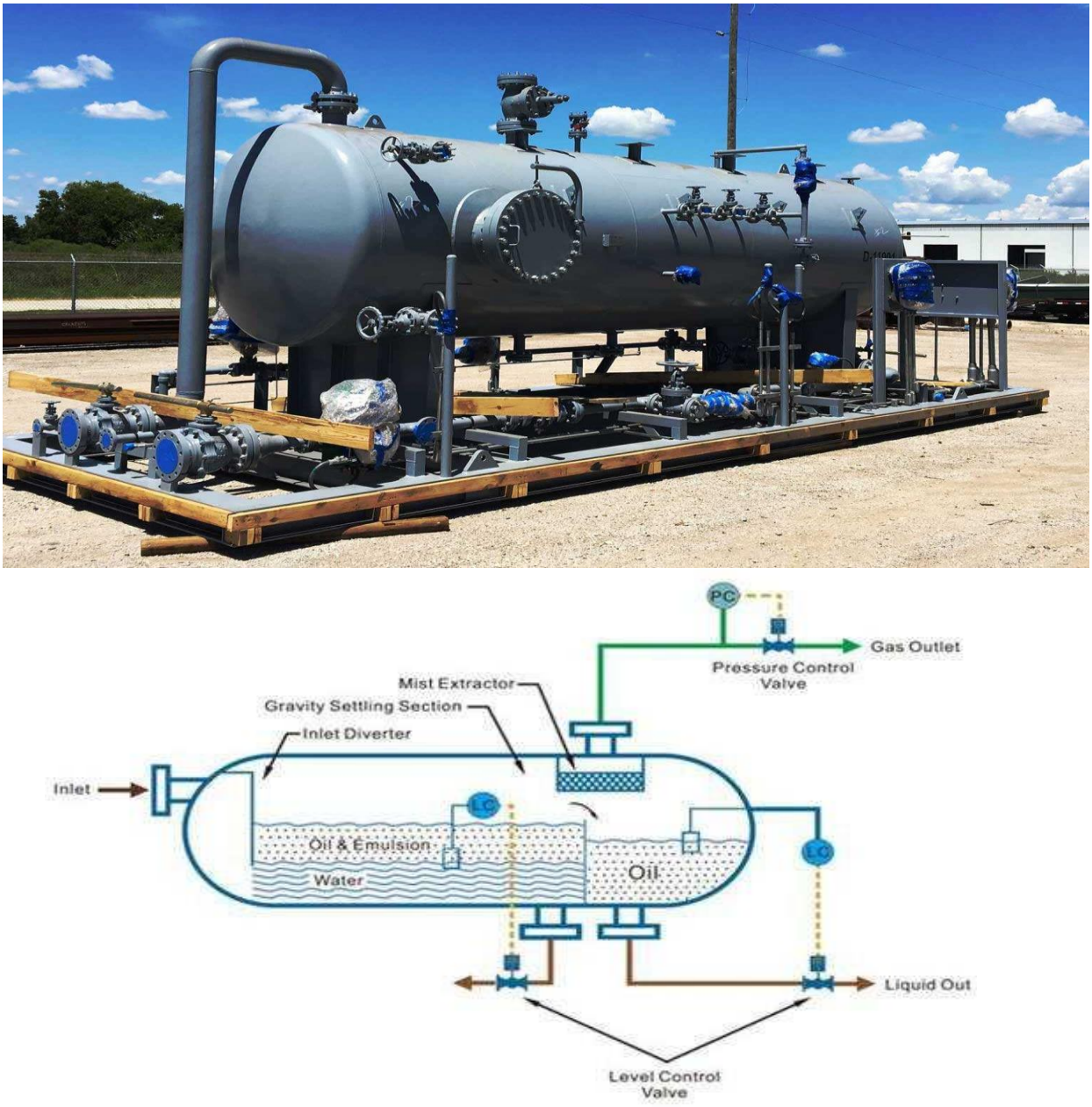

Figure I.2 Horizontal separator [2]

I.3.2.4 Spherical Separator

A spherical separator, as the name suggests, has a spherical shape as can be seen in Fig. I.3. It is used for the separation of liquids or gases and is particularly effective for high-pressure applications. The spherical shape allows for better distribution of stress and pressure, making it suitable for handling high-pressure fluids or gases. Also, it is less efficient than either horizontal or vertical cylindrical separators and is seldom used. Nevertheless, its compact size and ease of transportation have made it suitable for crowded processing areas and off-shore operations

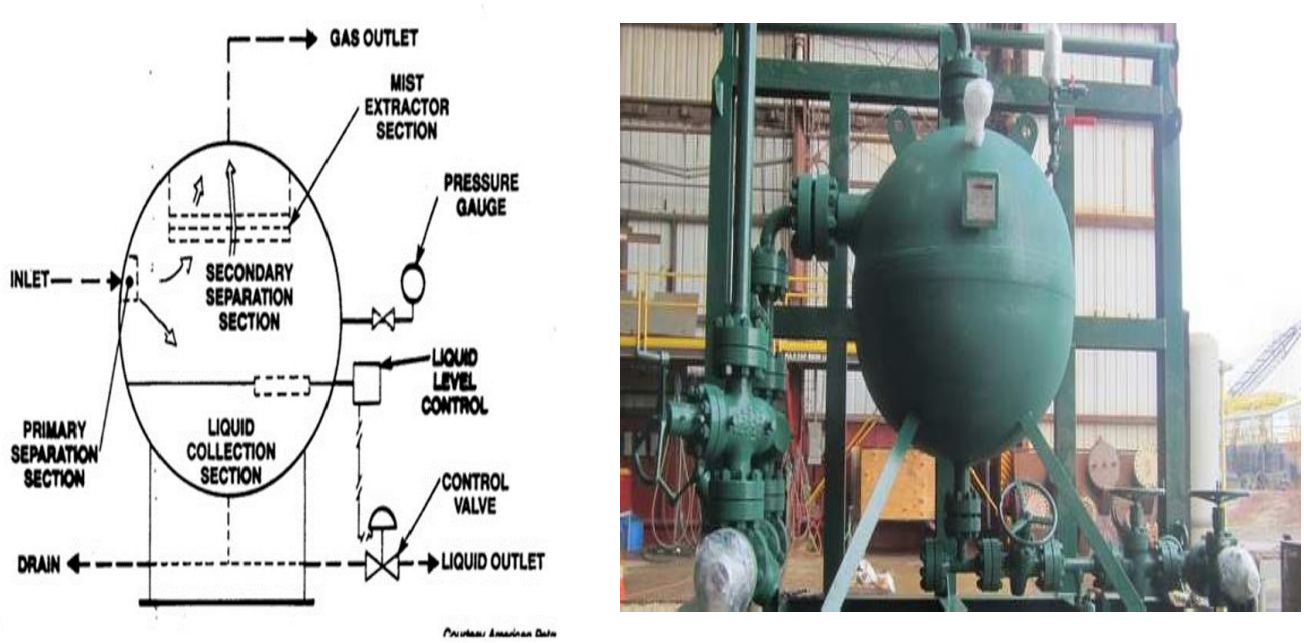

Figure I.3 Spherical separator [2]

Vertical, horizontal, and spherical separators each have their own advantages and are chosen based on factors such as the specific application, flow rate, pressure, and the characteristics of the substances being separated.

I.3.3 The difference between horizontal and vertical separators

Horizontal separators are smaller and less expensive than vertical separators for a given gas capacity. In the gravity settling section of a horizontal vessel, the liquid droplets fall perpendicular to the gas flow and thus are more easily settled out of the gas continuous phase. Also, since the interface area is larger in a horizontal separator than a vertical separator, it is easier for the gas bubbles, which come out of solution as the liquid approaches equilibrium, to reach the vapor space. Horizontal separators offer greater liquid capacity and are best suited for

liquid-liquid separation and foaming crudes. However, they do have some drawbacks that could lead to a preference for a vertical separator in certain situations:

1. Horizontal separators are not as good as vertical separators in handling solids.
2. Horizontal vessels require more plan area to perform the same separation as vertical vessels.
3. Smaller, horizontal vessels can have less liquid surge capacity than vertical vessels sized for the same steady-state flow rate.

I.3.4 Separator's equipments

Inside the separators we generally find the following main components: deflectors, coalescers, wiers, baffles, inlet diffusers, sand jet, and anti-surge baffles.

I.3.4.1 Deflector

Input deflector (Fig. I.4) is a device that deflects the incoming fluid stream onto a plate, causing a sudden change in direction and velocity. This helps to separate the larger liquid droplets from the gas phase by inertia and gravity.

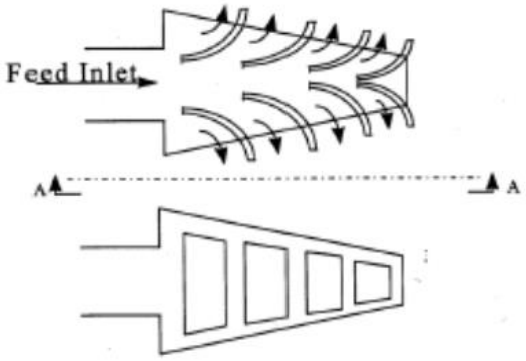

Figure I.4. Input deflector [7]

I.3.4.2 Coalescer

A coalescer (Fig. I.5) is a device that uses a porous material, such as wire mesh, vanes, or fibers, to make the small liquid droplets collide and merge into larger ones. This facilitates the separation of liquid and gas phases by gravity.

Figure I.5 Coalescer [7]

I.3.4.3 Plateau or weir

As depicted in Fig. I.6, a weir is a device that increases the residence ime of the liquid phase by increasing the volume available for it. It also helps to control the liquid level and flow rate in the separator

Figure I.6 Plateau or weir [6]

I.3.4.4 Baffles

Devices that reduce the turbulence in the gas stream after the initial separation by the deflector. They also act as collectors of liquid droplets and enhance the coalescence process. A typical baffle is illustrated in Fig. I.7.

Figure I.7 Baffles [5]

I.3.4.5 Inlet diffuser

A device that absorbs the kinetic energy of the incoming fluid stream, especially for oil wells. It can be centrifugal in vertical separators. The diffuser also provides a first stage of liquid-gas separation. Fig. I.8 shows a typical inlet diffuser.

Figure I.8 Inlet diffuser [3]

I.3.4.6 Sand jet

A device that allows the removal of sand accumulated with the liquids at the bottom of the separator. Water or chemicals are sent under pressure through this device. Sand jetting is often used before inspecting the separator. The picture of Fig. I.9 shows a typical sand jet.

Figure I.9 Sand jet [4]

I.3.4.7 Anti-surge baffles

As illustrated in Fig. I.10, these devices that prevent the propagation of waves at the liquid-gas interface in the separator. They are especially useful for separators mounted on floating platforms. They also reduce the settling lengths of liquids

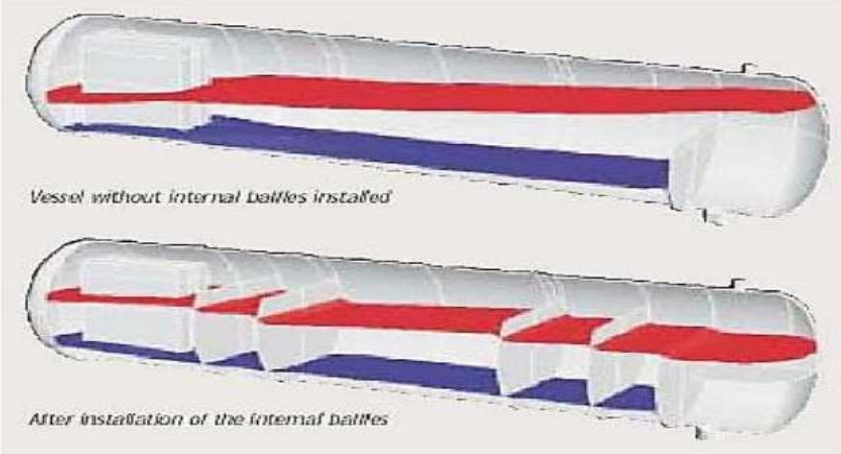

Figure I.10 Anti-surge baffles [9]

I.4 Industrial separators control

A separator usually has several control loops that control the pressure, level and temperature of the fluids inside the separator. The principles of control loops are based on the concepts of feedback and control. A feedback loop is a system that monitors the output of a

process and compares it with a desired set-point. A control loop is a system that adjusts the input of a process based on the feedback loop to maintain the output at the set point. Control loops are essential for ensuring the optimal performance and safety of a separator.

I.4.1 Principal control loops in the separators

In three-phase separators, it is essential to control the water level, oil level, and gas pressure. Consequently, there is typically a control loop for each of these variables. It is worth noting, however, that water level control in industrial separators is equally important and critical as in other technological processes. It directly influences the control loops for oil and gas pressure. The following sections will present certain control configurations installed in petroleum separators.

I.4.1.1 Water level control loop

This loop regulates the level of water in the separator vessel under the configuration shown in Fig. I.11. The water level control loop consists of a level transmitter (LT) which measures the water level, a controller (LC) which compares the measured level with a set point, and a control valve (LCV) which adjusts the flow of water to maintain the desired level.

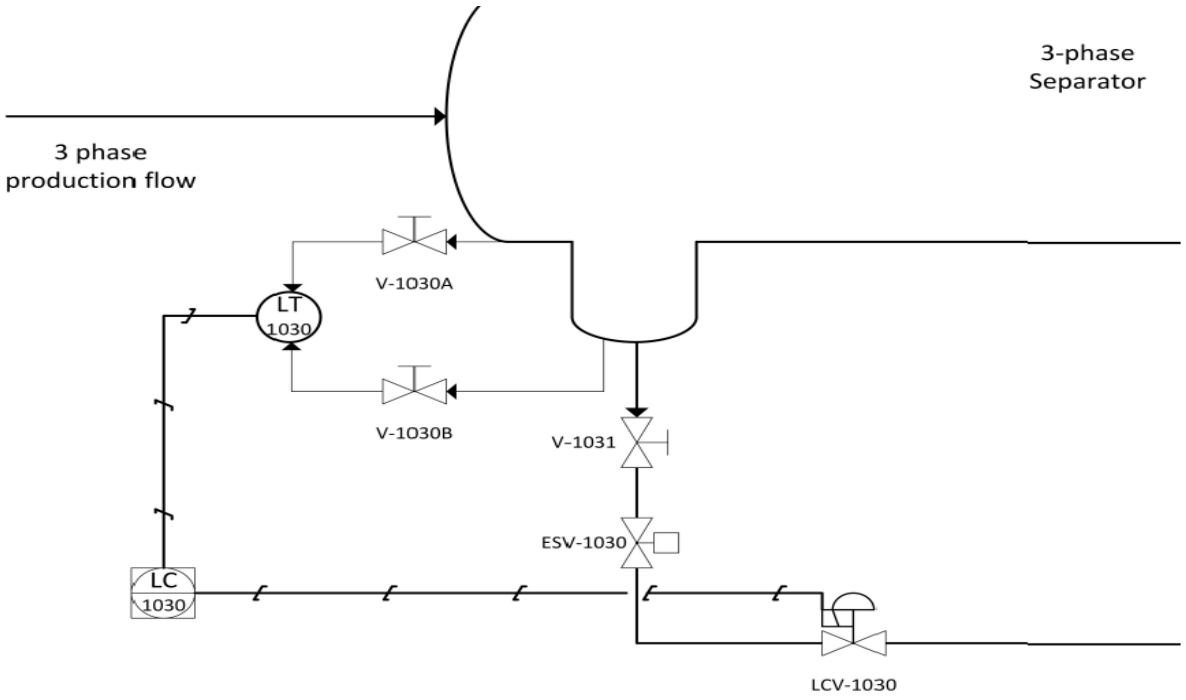

Figure I.11 Water level control loop in a three-phase separator [8].

I.4.1.2 Oil level control loop

The oil level in the separator vessel is controlled by this loop (see Fig. I.12). A level transmitter (LT) measures the oil level, a controller (LC) compares the measured level to a set point, and a control valve (LCV) modifies the flow of oil to maintain the desired level. These three components make up the oil level control loop.

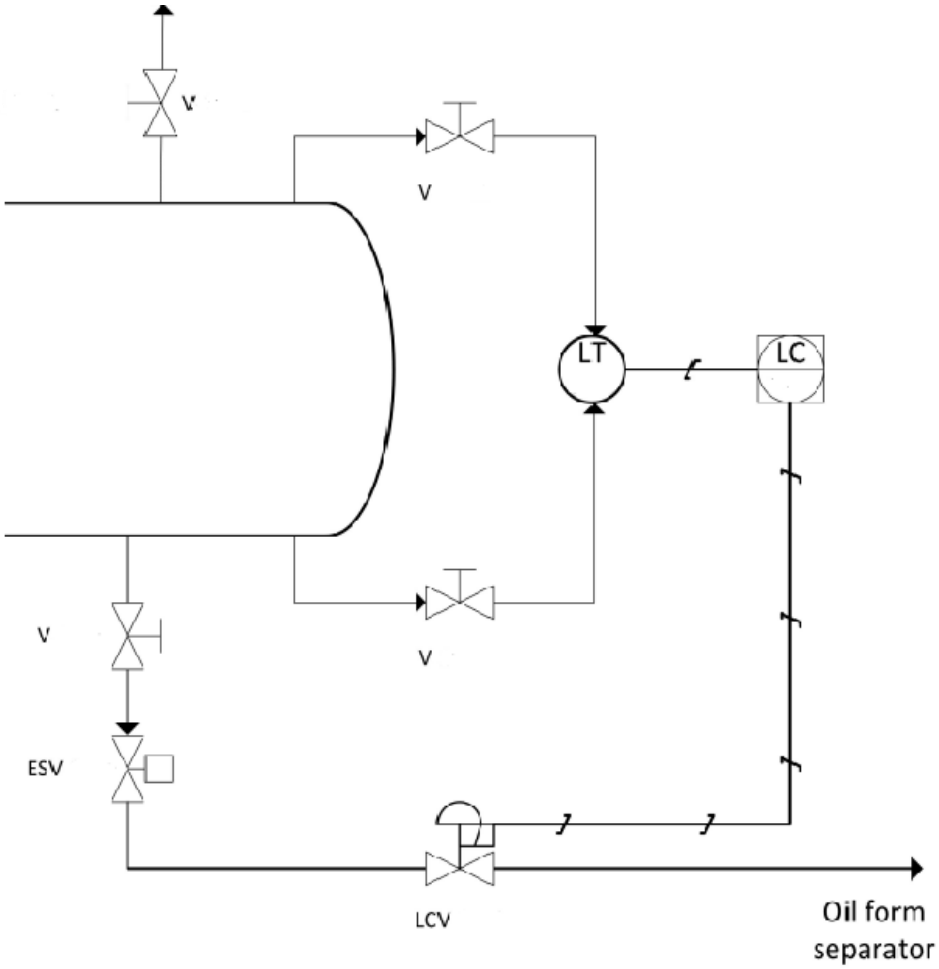

Figure I.12 Oil level control loop in a three-phase separator [8].

I.4.1.3 Gas pressure control loop

The separator vessel's gas pressure is controlled by this loop which is given in Fig. I.13. The components of the gas pressure control loop are a pressure transmitter (PT) for measuring gas pressure, a controller (PC) for comparing measured pressure to a set point, and a control valve (PCV) for adjusting gas flow to maintain the target pressure.

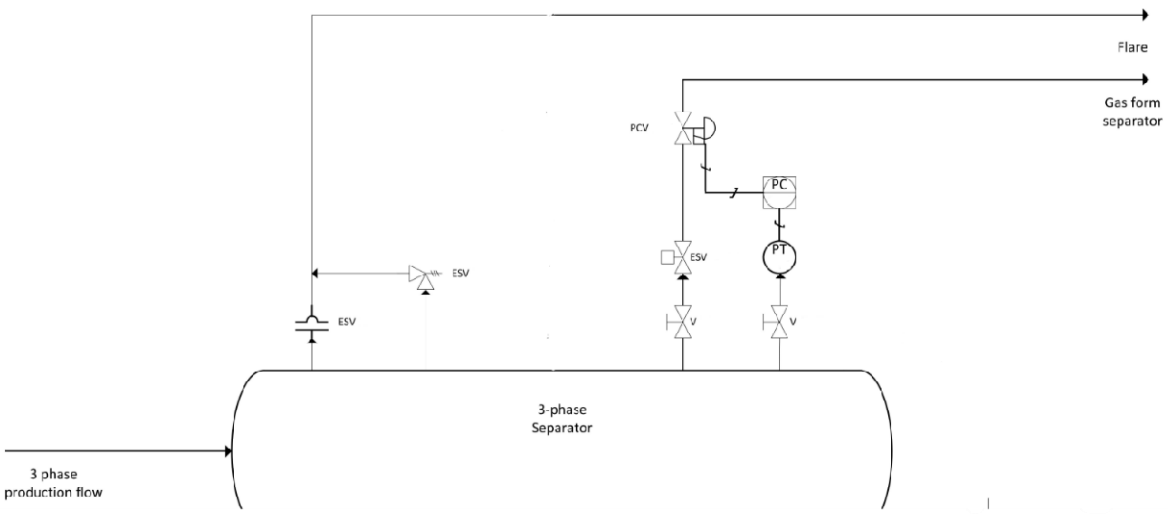

Figure I.13 Gas pressure control loop in a three-phase separator [8].

I.4.2 Control structures in a three-phase separator

There are different types of control schemes that can be used in a three-phase separator, depending on the desired control objectives and the process dynamics. Some examples are as follows.

I.4.2.1 PID control

This is a conventional method that uses proportional, integral and derivative actions to adjust the control valves for the liquid and gas outlets based on the measured levels and pressures in the separator. This method requires tuning the PID parameters to achieve satisfactory performance and stability.

I.4.2.2 Cascade control

This is a method that uses two nested PID loops for each control variable as depicted in Fig. I.14. The inner loop controls a fast variable, such as flow rate or valve position, while the outer loop controls a slow variable, such as level or pressure. This method can improve the response time and disturbance rejection of the system.

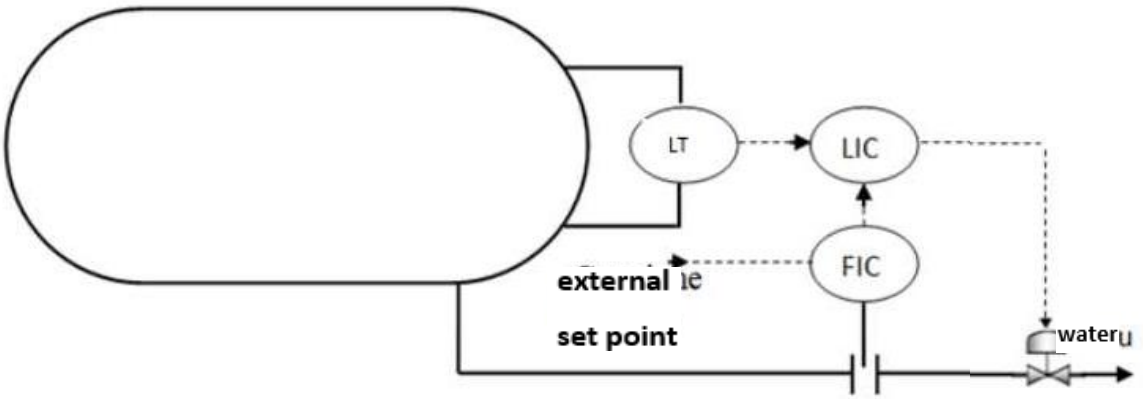

Figure I.14 Cascade control of water level in a separator.

I.4.2.3 Split-range control

This is a method that uses a single controller to manipulate two or more control valves with different ranges of operation (see Fig. I.15). For example, a split-range controller can regulate the gas pressure by opening a low-pressure valve when the pressure is below a certain set point, and opening a high-pressure valve when the pressure is above another set point. This method can handle nonlinearities and multiple operating conditions in the system.

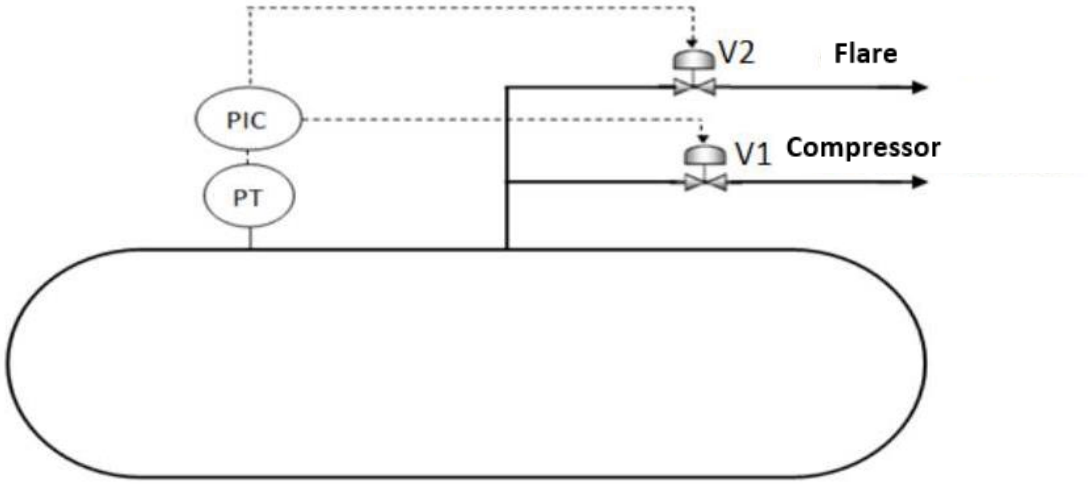

Figure I.15 Split-range control of gas pressure in a separator.

I.4.2.4 Auto-tuning control

This is a method that uses an adaptive mechanism to adjust the PID parameters automatically based on the process behavior and the control error. This method employs

advanced control protocols that help coping with uncertainties and variations in the system parameters and operating conditions

I.5 Conclusion

The separation process is a critical task in the oil and gas production units. Control loops are essential components of the separation process, as they help to maintain the desired process parameters for each phase of the fluid. From the description of multi-phase separators provided in this chapter, it can be easily concluded that this kind of oil production processes belong to the class of highly complex systems that require stringent monitoring and control to ensure optimal operation and performance. By using advanced technologies and sophisticated control systems, the separation process can be optimized to improve efficiency, reduce costs, and enhance the quality of the separated fluids.

CHAPTER II Description and modeling of the 10-V-255 three-phase separator

II.1 Introduction

Efficient separation of fluids in oil production separators can only be ensured by a good functioning of the associated equipments including the system and control parts. It is the aim of the regulatory parts to maintain the different process variables within their admissible ranges while dealing with the sudden changes in process operation and severe disturbances.

The separation process under study is a three-phase separator of horizontal type, part of oil production facility. In order to address its control problem, we first need to detail its physical structure and get better insight about its dynamical behavior with the aim to construct a feasible model that can be used for control design. This chapter addresses the issue of modeling of the three-phase separator 10-V-255, where we describe the complete procedure of physical modeling of the system and present the associated control loops.

II.2 Process description

The separator 10-V-255 (Fig. II.1) is a unit located in a centre called GS1 which is a collection field for oil production from the entire site (GS-1, the ARs, and ZOTTI). The crude oil is transported via pipelines to Haoud-EL-Hamra "H.E.H". Of course, passing through separators is essential for its treatment, and then the oil is placed in tanks awaiting the shipment operation.

Figure II.1 GS1 overview.

II.2.1 Technical specifications

Size:	2435 mm ID x 7315 mm S/S
Design:	18.48 barg (271.65psi) at temperature from -10/75°C temp.
Operating Pressure:	1.5 barg to 2.5 barg at 30°C/40°C max.
Separator Capacity:	50,700 BFPD
	(Maximum oil phase 28,700 & max. water phase 22,000 BWPD)
Gas Capacity:	75 MMSCFD

The separator is controlled by the Distributed Control System DCS ALLEN-BRADLEY PANEL VIEW 1010 illustrated in Fig. II.2. The DCS system is located in the new control room. The DCS controls all PETROFAC separator parameters of pressure and levels. Also, the DCS receives and sends signals to the separator instrument devices.

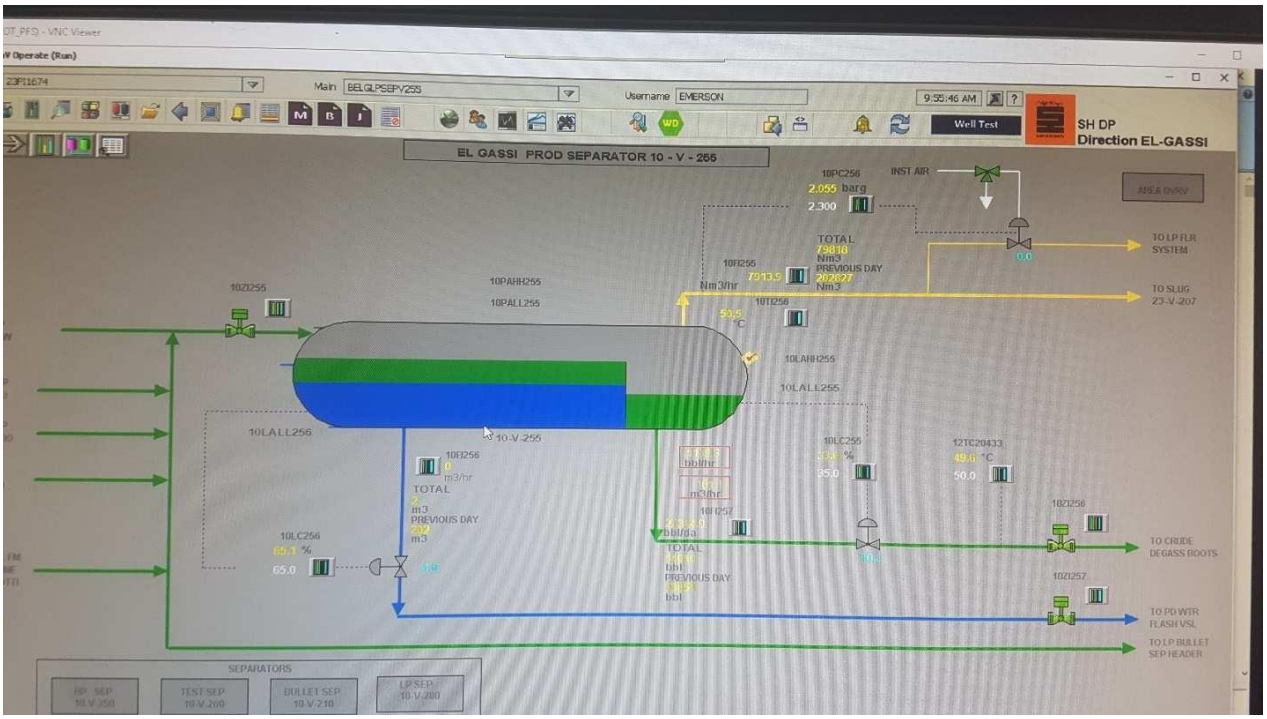

Figure II.2 Distributed Control System of the 10-V-255 separator.

II.2.2 Process components and operation

II.2.2.1 Separator inlet

Oil enters the separator from the following sources:

1. EL-GASSI high pressure PETROFAC separator (10-V-250) 6-inch oil outlet line.

2. PETROFAC test separator (10-V-260). The 3-inch oil outlet line.
3. High pressure separators (10-V-200) 6-inchoil outlet line.
4. West EL-AGREB 18-inch line with ZOTTI.

Oil production through the new 10”x12”.

Both lines are combined together at GS-1 production pig receivers’ area.

These lines are connected together in one 14-inch inlet line.

The inlet line is equipped with 10-inch ESDV-255.

The 10-inch ESDV-255 is activated by the following signals; the Emergency Shut-down

Bottom ESDB, PSHH – 255&LSHH-255.

II.2.2.2 Gas outlet

The separated gas exits the separator through the gas outlet 6-inch line. The gas passes through the orifice plate, i.e. flow element. The gas outlet line then splits into two branches. The first branch (6”-HV-324-BIG) sends gas to the EGI. The Second branch which is equipped with 6-inch pressure control valve (fail open) sends surplus gas to low pressure Knock-out drum before flowing to the low pressure flare. Currently the separator operating pressure is 2.5 barg.

In case of the separator receiving a shut-down signal from the PCV-256 will fall open, also the EGI plant will be down due to insufficient supply of gas and Vapor Recovery Unit (RVU) as well.

Second stage separator alarms (LSHH) activates the inlet ESDVs of high pressure separator PETROFAC (10-V-250) and PETROFAC test separator (10-V- 60).

II.2.2.3 Oil outlet

Oil exits the separator through the 10-inch oil outlet line. The Oil flows through the permanent strainer then flows to turbine flow meter, then through the level control valve, and finally through the 10-inch oil outlet ESDV-256. The ESDV-256 is activated by the following signals: oil LSLL-255, interface LSLL-255 and ESDB.

II.2.2.4 Water outlet

The produced water exits the separator through the 2-inch water outlet line then flows to the permanent strainer, the 2-inch water turbine meter, water level control valve, the (ESDV-256) and finally water flows to the evaporate pond. The ESDV-257 is activated by these signals: LSLL-255, LSHH-255 and ESDB.

The water outlet system is equipped with sand trap in which sand is trapped to be dumped while the separator is in service.

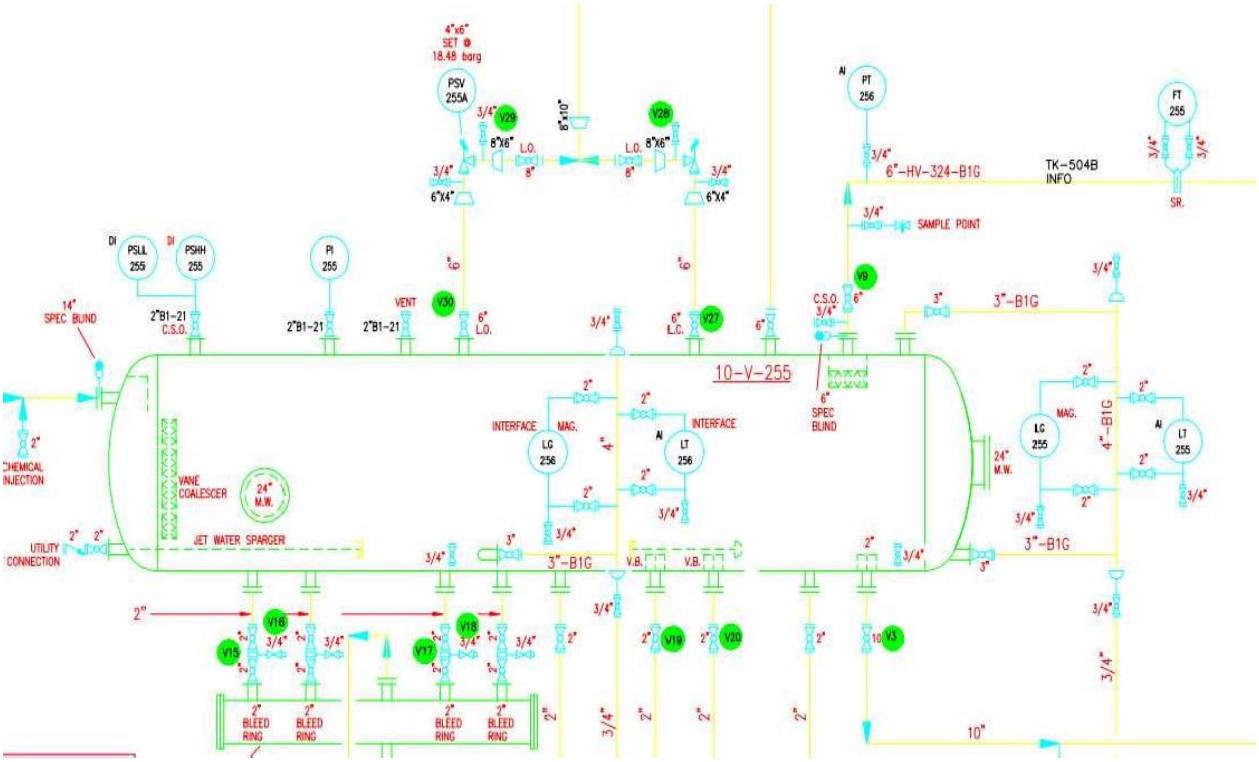

Figure II.3 Piping and instrument diagram of the 10-V-255 separator.

II.3 Separator modeling

The process of separation being analyzed involves three process vari bles that can be measured: gas pressure, oil level, and water level. The model for each state is based on physical laws and the geometry of the separator. We resorted in this report to the ork by [**10**] for building a reliable model for the three-phase separator under study as it studies on similar separator models. The model presented in this report does not consider flashing, but it is accounted for in the mass balance equation. In the process analyzed in this task, the net inflow is

equal to the net outflow for each component. Flashing is denoted as a factor Z in the mass balance model. In the analysis conducted by [10] transients caused by flashing are discussed

A separator is commonly built as a horizontal cylinder, which is also the case for the plant being analyzed. The section designated for oil is assumed to have smooth walls. However, for the separator being considered in this report, only the separator geometry is taken into account, while the end sections are assumed to have smooth walls. If the separator is short and has a large radius, the curved end sections, which are present in most cases, should be considered.

The three-phase (10-V-255) separator is a horizontal vessel with a diameter of 2,435 meters and 7,315 meters length. The orientation and geometry of the separator are optimized to separate a fluid stream into three phases: oil, gas, and water.

The surface of a liquid can vary depending on the level of the liquid, and we can use Equation II-1which follows the Pythagoras formula, to calculate the width of the liquid surface. This equation takes into account parameters such as half of the width, indicated by β, the radius denoted by r, the liquid level represented by h, and the distance between the liquid level and the center of the tank, called α [11]. Figure II.4 displays a diagram of the separator cross-section, including the parameters of interest.

$$r^2 = \alpha^2 + \beta^2 \qquad \text{II -1}$$

$$\beta^2 = r^2 - \alpha^2 \qquad \text{II -2}$$

$$\beta = \sqrt{r^2 - \alpha^2} \qquad \text{II -3}$$

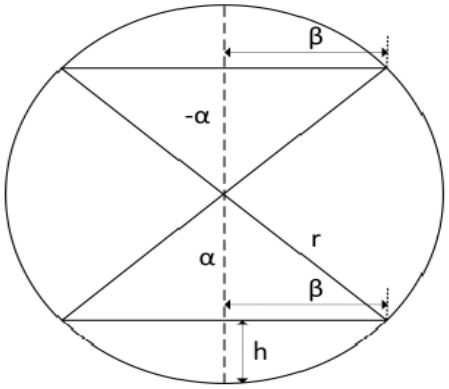

Figure II. 4 The separator cross-section.

In Equation II-3 we change α to r − h to make β as a function of h shown in Equation II-4 and Equation II-5.

$$\beta(h) = \sqrt{r^2 - (r-h)^2} \quad \text{II-4}$$

$$\beta(h) = \sqrt{2rh - h^2} \quad \text{II-5}$$

It appears that there may be issues if the liquid level surpasses the midpoint of the separator, resulting in a negative value for α, which is not allowed in the calculations. Nevertheless, this problem can be resolved through symmetrical considerations, to prove that the calculations still function properly even with a negative α. The formula for determining the width of the liquid surface enables us to calculate the area of the cross-section, which can be achieved by integrating the line segments from the bottom of the separator, h = 0, up to the liquid level. The area of the liquid cross-section is referred to as A(h).

$$A(h) = 2 \cdot \int_0^h \sqrt{2rh' - h'^2}\, dh' \quad \text{II-6}$$

$$A(h) = 2 \cdot \int_0^h \sqrt{\beta(h')}\, dh' \quad \text{II-7}$$

To determine the volume of the liquid, we can multiply the cross-sectional area by the length, l, of the section designated for the liquid. Equation II-8 can be used to calculate the derivative of volume. Figure II.5 displays the construction and dimensions of the tank, which are necessary for volume calculation.

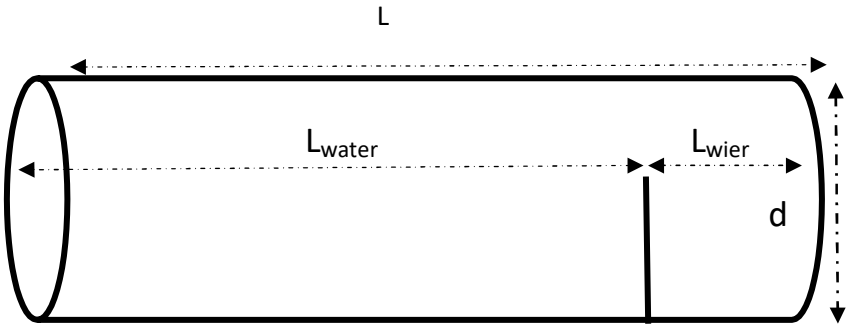

Figure II.5 The geometry of the separator

$$V(h) = 2l \cdot \int_0^h \beta(h')\, dh' \quad \text{II-8}$$

$$\frac{dV}{dt} = \frac{d}{dt}\left(2l \cdot \int_0^h \beta(h')\, dh'\right) \quad \text{II-9}$$

$$\frac{dV}{dt} = \frac{6}{6t}(2l \cdot \int_0^h \beta(h')dh')\frac{6h}{6t} \quad \text{II-10}$$

$$\frac{dV}{dt} = 2l(\beta(h) - \beta(0))\frac{6h}{6t} \quad \text{II-11}$$

UNITS	DIMENSION
LENGTH	l = 7,135m
WATER COMPARTMENT LENGTH	l_w = 4,982m
DIAMETER	D = 2,435
WEIR LENGTH	l_{wier} = 1,930m
WATER LEVEL SETPOINT	h_{wsp} = 0,462m
OIL LEVEL SETPOINT	h_{osp} = 1,26m
GAS PRESSURE SETPOINT	P_{gsp} = 2,1 bar

Table II-1Actual dimensions of the separator 10-V-255 and nominal operating conditions.

II.3.1 Water level model

The liquid level can be determined by utilizing mass balance, which is outlined in studies conducted by [10] as well as [11]. Equation II-15 can be used to calculate the change in water level from the mass balance. We can examine the water mass flow that is introduced into the process, ω_{i_w}, and the water mass flow that exits the process, ω_{o_w}. The term Z_w represents the process of flashing.

$$\frac{dm_w}{dt} = \omega_{i_w}(t) - \omega_{o_w}(t) - Z_w \quad \text{II-12}$$

$$\frac{dV_w}{dt}\rho_w = \rho_w(q_{i_w}(t) - q_{o_w}(t)) - Z_w \quad \text{II-13}$$

Assuming that the water density, ρ_w, is constant results in a constant volume. The net water volume flow, which is the difference between the inflow and the outflow ($q_{iw}(t)$ - $q_{ow}(t)$) of water, is referred to as $q_w(t)$. As the analysis does not consider flashing, Z_w is not utilized in any subsequent calculations.

$$\frac{dV_w}{dt} = q_{i_w}(t) - q_{o_w}(t) \quad \text{II-14}$$

$$\frac{6}{6h_w}(2l \cdot \int_0^{h_w} \beta(h')dh') \cdot \frac{dh_w}{dt} = q_{i_w}(t) - q_{o_w}(t) \quad \text{II-15}$$

$$\frac{dh_w}{dt} = \frac{6}{6h_w(2l\cdot\int_0^{h_w}\beta(h)dh)}q_w(t) \quad \text{II-16}$$

$$\frac{dh_w}{dt} = \frac{1}{2l(\beta(h_w)-\beta(h_0))}q_w(t) \quad \text{II-17}$$

Equation II-17 represents the differential equation that expresses the alteration in water level. In order to analyze the system, it would be beneficial to convert the model into the frequency domain, as indicated in the calculations from Equation II-18. However, because our model is nonlinear, we must first linearize the model before we can create a transfer function. Ideally, we want to linearize the model around the water level set point h_{wsp}.

$$f\{\frac{dhw}{dt}\} = f\{\frac{1}{2l\cdot\beta_w(h_{w_{sp}})}\cdot(q_w(t))\} \quad \text{II-18}$$

$$sh_w(s) = \frac{q_w(s)}{2l\cdot\beta_w(h_{w_{sp}})} \quad \text{II-19}$$

$$h_w(s) = \frac{q_w(s)}{2l\cdot\beta_w(h_{w_{sp}})s} \quad \text{II-20}$$

$$h_w(s) = \frac{q_w(s)}{2l\cdot(\sqrt{2rh_{w_{sp}} - h_{w_{sp}}{}^2})s} \quad \text{II-21}$$

$$2l_w\cdot(\sqrt{2rh_{w_{sp}} - h_{w_{sp}}{}^2}) = 9{,}51 \quad \text{II-22}$$

$$h_w(s) = \frac{1}{9{,}51s}q_w(s) = \frac{10{,}51\times10^{-2}}{s}\cdot q_w(s) \quad \text{II-23}$$

In order to analyze the nonlinear system, it is necessary to perform linearization around various values of β(h). Nonlinearity in the system may cause some undesired effects.

II.3.2 Oil level model

Next, we will derive the model for the oil level. We will examine the oil level, h_o, in relation to the water level, h_w. Initially, we will determine the available volume of oil in the separator, knowing that the oil volume is partitioned into three sections, which are mathematically defined in Equation II-24. The space between the water level and the top of the weir has a length of l_w. The length from the top of the weir to the oil surface is l, and the length from the bottom of the separator to the top of the weir is $l - l_w$. In our model, the oil level must

not fall below the top of the weir. Consequently, the oil volume in the chamber beneath the weir and on the outflow side can be considered a constant value. It is understood that the oil level is influenced by the water level.

From Figure II.4 and Figure II.5, we can see that the oil level is dependent of water level.

$$V_{\mathrm{o}}(h_{\mathrm{w}}, h_{\mathrm{o}}) = V(h_{\mathrm{o}}) + V(h_{\mathrm{w}}) + V_{\mathrm{wier}} \quad \text{II-24}$$

$$\frac{dV_o(h_{\mathrm{w}},h_o)}{dt} = \frac{6V_o}{6h_{\mathrm{w}}}\frac{dh_{\mathrm{w}}}{dt} + \frac{6V_0}{6h_o}\frac{dh_o}{dt} \quad \text{II-25}$$

$$\frac{dV_o(h_{\mathrm{w}},h_o)}{dt} = \frac{6V_{o1}}{6h_{\mathrm{w}}}\frac{dh_{\mathrm{w}}}{dt} + \frac{6V_{o2}}{6h_o}\frac{dh_o}{dt} \quad \text{II-26}$$

$$V_{\mathrm{o1}} = 2l_{\mathrm{w}}\int_{h_{\mathrm{w}}}^{h_{\mathrm{wier}}}\beta(h')dh' \quad \text{II-27}$$

$$\frac{6V_{o1}}{6h_{\mathrm{w}}} = 2l_{\mathrm{w}}\frac{6}{6h_{\mathrm{w}}}(\beta(h_{\mathrm{wier}}) - \beta(h_{\mathrm{w}})) \quad \text{II-28}$$

$$\frac{6V_{o1}}{6h_{\mathrm{w}}} = 2l_{\mathrm{w}}\frac{6}{6h_{\mathrm{w}}}(-\beta(h_{\mathrm{w}})) \quad \text{II-29}$$

$$V_{\mathrm{o2}} = 2l\int_{h_{\mathrm{wier}}}^{h_o}\beta(h')dh' \quad \text{II-30}$$

$$\frac{6V_{o2}}{6h_{\mathrm{w}}} = 2l\frac{6}{6h_o}(\beta(h_{\mathrm{o}}) - \beta(h_{\mathrm{wier}})) \quad \text{II-31}$$

$$\frac{6V_{o2}}{6h_{\mathrm{w}}} = 2l\frac{6}{6h_o}(\beta(h_{\mathrm{o}})) \quad \text{II-32}$$

The change in oil level is derived from mass balance given in Equation II-33. Flashing is denoted as $Z_{o.}$

$$\frac{dm_o}{dt} = \omega_{\mathrm{i}_o}(t) - \omega_{\mathrm{o}_o}(t) - Z_{\mathrm{o}} \quad \text{II-33}$$

$$\frac{dV_o}{dt}\rho_{\mathrm{o}} = \rho_{\mathrm{o}}(q_{\mathrm{i}_o}(t) - q_{\mathrm{o}_o}(t)) - Z_{\mathrm{o}} \quad \text{II-34}$$

Assuming that the oil density, ρ_o, is constant, we can continue with the calculations for volume flow. The process of flashing, Z_o, is not considered in the analysis and is not used in any subsequent calculations. The net oil flow is referred to as $q_o(t)$, which is the difference between the inflow ($q_{io}(t)$) and outflow ($q_{oo}(t)$) of oil.

Oil volume given in Equation II-29 and Equation II-32 put together with mass balance, leads to the model for oil level change given in Equation II-38.

$$\frac{dV_o}{dt} = q_{i_o}(t) - q_{o_o}(t) \quad \text{II-35}$$

$$\frac{6V_{o1}}{6h_w}\frac{dh_w}{dt} + \frac{6V_{o2}}{6h_o}\frac{dh_o}{dt} = q_{i_o}(t) - q_{o_o}(t) \quad \text{II-36}$$

$$\frac{6V_0}{6h_o}\frac{dh_o}{dt} = q_{i_o}(t) - q_{o_o}(t) - \frac{6V_o}{6h_w}\frac{dh_w}{dt} \quad \text{II-37}$$

$$\frac{dh_o}{dt} = \frac{q_{i_o}(t) - q_{o_o}(t) - \frac{67_o}{6h_w}\frac{dh_w}{dt}}{\frac{67_0}{6h_o}} \quad \text{II-38}$$

Similar to the water level, we will transform the system into the frequency domain for analytical purposes. In order to create a transfer function, we need to linearize the system presented in Equation II-38 around a working point. For simplicity, we will assume that the water level is constant with a value of k_w at the working point during analysis. Equation II-39 represents the linearized model of the oil level in the time domain.

$$h_o(s) = \frac{q_o(s) - 2l(\beta(h_{w_{sp}})\cdot k_w)}{2l\beta(h_{o_{sp}})s} \quad \text{II-39}$$

In the expression $2l\beta\ (h_{w_{sp}})\ k_w$, the term k_w represents the impact of changes in water level on the level of oil in the separator. As a result, it will be treated as a variable that causes disturbances in order to take into account its effect on the oil level. This simplifies the model, which can be expressed in the following form.

$$h_o(s) = \frac{q_o(s)}{2l\beta(h_{o_{sp}})s} \quad \text{II-40}$$

$$2l\beta\ (h_{o_{sp}}) = 2l\sqrt{2rh_{o_{sp}} - h_{o_{sp}}^{\ 2}} \quad \text{II-41}$$

$$2l\sqrt{2rh_{o_{sp}} - h_{o_{sp}}^{\ 2}} = 17{,}80 \quad \text{II-42}$$

$$h_o(s) = \frac{q_o(s)}{17{,}80s} = \frac{5{,}62\times10^{-2}}{s}\cdot q_o(s) \quad \text{II-43}$$

II.3.3 Gas pressure model

The pressure of gas in the separator is influenced by the volume of gas available, the balance of mass, and the density of gas. Although gas pressure is also affected by temperature and flashing, these factors are not considered in this analysis, even though flashing is shown in the mass balance equation. We will now establish the model for gas pressure, beginning with the definition of the volume of gas available and the derivative of gas volume.

$$V_{\mathrm{g}}(h_{\mathrm{o}}) = 2l\int_{h_o}^{2r}\beta(h')dh' \qquad \text{II-44}$$

$$\frac{6V_g}{6h_o} = \frac{6}{6h_o}(\beta(2r) - \beta(h_{\mathrm{o}})) \cdot 2l \qquad \text{II-45}$$

$$\frac{6V_g}{6h_o} = -\beta(h_{\mathrm{o}}) \cdot 2l \qquad \text{II-46}$$

$$\frac{dV_g}{dt} = \frac{6V_g}{6h_o}\frac{6h_o}{6t} \qquad \text{II-47}$$

$$\frac{6V_g}{6h_o} = -2l \cdot \beta(h_{\mathrm{o}}) \cdot \frac{dh_o}{dt} \qquad \text{II-48}$$

Because the volume of the process is not consistent, a volume balance cannot be utilized in the calculation. However, a mass balance can be employed to model the process, using the ideal gas law (as presented in Equation II-49) and the mass balance (as presented in Equation II-50) as the foundation for our model. If necessary, flashing can be incorporated by including the Zg factor in the mass balance equation II-50, but in this instance, it is not considered in subsequent calculations.

$$pV_{\mathrm{g}} = m_{\mathrm{g}}RT \qquad \text{II-49}$$

$$\frac{dm_g}{dt} = \omega_{\mathrm{i}_g}(t) - \omega_{\mathrm{o}_g}(t) - Z_{\mathrm{g}} \qquad \text{II-50}$$

The gas density is not constant, therefore a differential equation for gas density is needed. The gas is considered as a perfect gas, which allows us to write:

$$m_{\mathrm{g}} = \rho_{\mathrm{g}}V_{\mathrm{g}} \qquad \text{II-51}$$

$$pV_{\mathrm{g}} = m_{\mathrm{g}}RT \qquad \text{II-52}$$

$$p = \rho_g RT \quad \text{II-53}$$

$$\frac{dp}{dt} = \frac{d\rho_g}{dt} RT \quad \text{II-54}$$

$$\frac{d\rho_g}{dt} = \frac{1}{RT} \cdot \frac{d}{dt} \quad \text{II-55}$$

We have obtained the derivative of mass, assuming a constant temperature in the separator. The resulting equation that describes the variation in gas pressure is presented as Equation II-55

$$\frac{dm_g}{dt} = \frac{d\rho_g}{dt} V_g + \frac{dV_g}{dt} \rho_g \quad \text{II-56}$$

$$\frac{dm_g}{dt} = \frac{V_g\, dp}{RT\, dt} + \rho_g \frac{dV_g}{dt} \quad \text{II-57}$$

$$\frac{dm_g}{dt} = \frac{V_g\, dp}{RT\, dt} + \frac{p\, dV_g}{RT\, dt} \quad \text{II-58}$$

$$\omega_{i_g}(t) - \omega_{o_g}(t) = \frac{V_g\, dp}{RT\, dt} + \frac{p\, dV_g}{RT\, dt} \quad \text{II-59}$$

$$\frac{dp}{dt} = RT \left(\frac{\omega_{i_g}(t) - \omega_{o_g}(t)}{V_g} \right) - p \frac{\frac{d7_g}{dt}}{V_g} \quad \text{II-60}$$

Letting

$$\omega_{i_g}(t) - \omega_{o_g}(t) = \omega_g(t) \quad \text{II-61}$$

$$\frac{dp}{dt} = RT \left(\frac{\omega_g(t)}{V_g} \right) - p \frac{\frac{d7_g}{dt}}{V_g} \quad \text{II-62}$$

with

$$\frac{dV_g}{dt} = \frac{6V_g}{6h_o} \cdot \frac{6h_o}{6t} \quad \text{II-63}$$

$$\frac{dp}{dt} = RT \left(\frac{\omega_g(t)}{V_g} \right) - p \frac{\frac{67_g}{6h_o} \cdot \frac{6h_o}{6t}}{V_g} \quad \text{II-64}$$

As a simplifying assumption, it is assumed that the variation in gas volume is independent of the variation in oil level. The term $\frac{6V_g}{6h_o}$ then acts as a disturbance variable on the gas pressure, resulting in:

$$\frac{dp}{dt} = RT \cdot \frac{\omega_g(t)}{V_g} \quad \text{II-65}$$

$$sp(s) = RT \cdot \frac{\omega_g(s)}{V_g} \quad \text{II-66}$$

$$p(s) = \frac{RT}{V_g.s}\omega_{\mathrm{g}}(s) \quad \text{II-67}$$

with $V(h_{\mathrm{o}}) = 2l\int_{h_o}^{2r}\beta(h)dh$ is the volume dedicated as a reference level for the oil when oil level equal to oil level setpoint $h_{\mathrm{o}} = h_{osp}$. Having V_g=17,56 m^3, we get:

$$p(s) = \frac{147,25}{s}\omega_{\mathrm{g}}(s) \quad \text{II-68}$$

II.4 Valve actuators modeling

Automatic valves are used to control the separator variables, including the levels of water and oil and the pressure of the gas. Additionally, these actuators are designed to be incorporated into the calculations for regulating the system.

II.4.1 Model of an automatic valve

Typically, valves are represented by a mathematical formula that describes their behavior, which includes a time delay τ that accounts for the time it takes for fluid to flow through the pipe and a time constant T. Valves of a larger size frequently exhibit both a time constant and a time delay. In this specific facility, liquid valves have a dead band value of τ = 5 seconds and a time constant of T = 6 seconds, which is modeled using a first-order dynamic equation II-69. The assumption is made that both valves and pipes have no friction. Equation II-71 provides the valve equation in the time domain for the nonlinear valve that has been linearized around a working point z_{wp}, with the gas pressure set at a specific point p_{sp} [12].

$$h_a(s) = \frac{1}{T_a s+1} \cdot \mathrm{e}^{-cs} \quad \text{II-69}$$

$$q_{\mathrm{o}}(s) = \frac{\mathrm{k}_v \mathrm{f}(z_{wp})}{T_a s+1} \mathrm{e}^{-cs} \quad \text{II-70}$$

$$h_a(s) = \frac{q}{T_a s+1} \cdot \mathrm{e}^{-cs} \quad \text{II-71}$$

$$h_a(s) = \frac{q}{6s+1} \cdot \mathrm{e}^{-5s} \quad \text{II-72}$$

II.4.2 Water valve model

The transfer function of the water level control valve is of the form:

$$h_{a_{\mathrm{w}}}(s) = \frac{q\mathrm{w}}{T_a s+1} \cdot \mathrm{e}^{-cs} \quad \text{II-73}$$

with $$q_{\mathrm{w}} = 1501\ BPD = 1{,}842 \times 10^{-3} m^3/s \quad \text{II-74}$$

Knowing that : $$1BPD(barrel\ per\ day) = 1.84 \times 10^{-6}\ m^3/s \quad \text{II-75}$$

$$h_{a_{\mathrm{w}}}(s) = \frac{1{,}842\times10^{-3}}{6s+1} \cdot \mathrm{e}^{-5s} \quad \text{II-76}$$

II.4.3 Oil valve model

$$h_{a_{\mathrm{o}}}(s) = \frac{qo}{6s+1} \cdot \mathrm{e}^{-5s} \quad \text{II-77}$$

with $$q_{\mathrm{o}} = 39039\ BPD = 7{,}184 \times 10^{-2} m^3/s \quad \text{II-78}$$

$$h_{a_0}(s) = \frac{7{,}184\times10^{-2}}{6s+1} \cdot \mathrm{e}^{-5s} \quad \text{II-70}$$

II.4.4 Gas valve model

There is no time delay modeled for the gas actuator, although there may be some small delay present. However, this delay is negligible when compared to the time constant. For the valve being used in this specific case, the time constant is T_g = 60 seconds.

$$h_{a_g}(s) = \frac{K_g}{T_g.s+1} \quad \text{II-80}$$

with $$K_{\mathrm{g}} = 2.5\ MMSCFD = 0.8175\ m3/s \quad \text{II-81}$$

$$h_{a_g}(s) = \frac{0.8175}{60.s+1} \quad \text{II-82}$$

Knowing that MMSCFD stands for "Million Standard Cubic Feet per Day" and is a unit of measurement commonly used in the oil and gas industry to measure the flow rate of natural gas or other hydrocarbons. It is frequently abbreviated as MMSCFD and is used to represent the volume of gas extracted, processed or transported in large quantities.

II.5 Control loops of the separator

The statement suggests that a control system is being proposed for the separator equipment, which will comprise a sensor, a regulating valve, and a regulator. This system is intended to regulate various parameters such as water level, oil level, and gas pressure, to ensure that they remain within acceptable limits during normal operation.

II.5.1 Water level control loop

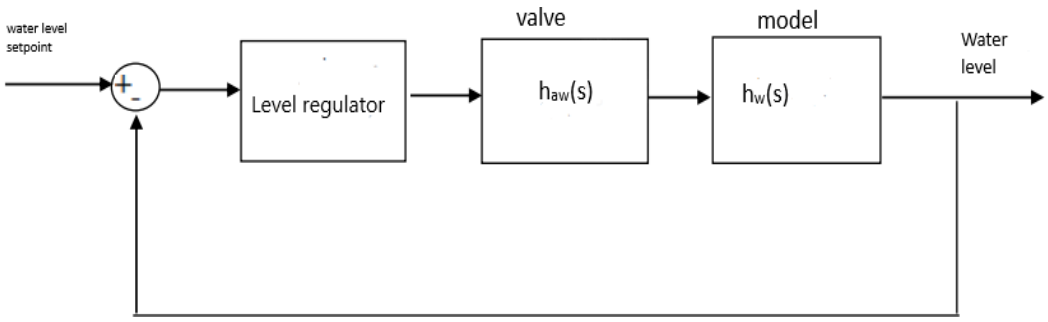

Figure II.6 Water level control loop.

The transfer function of the water level control loop is given by:

$$H_{\mathrm{w}}(s) = h_{\mathrm{w}}(s).h_{a_{\mathrm{w}}}(s) \quad \text{II-83}$$

$$H_{\mathrm{w}}(s) = \frac{1.936.10^{-4}}{s(6s+1)}.\mathrm{e}^{-5s} \quad \text{II-84}$$

II.5.2 Oil level control loop

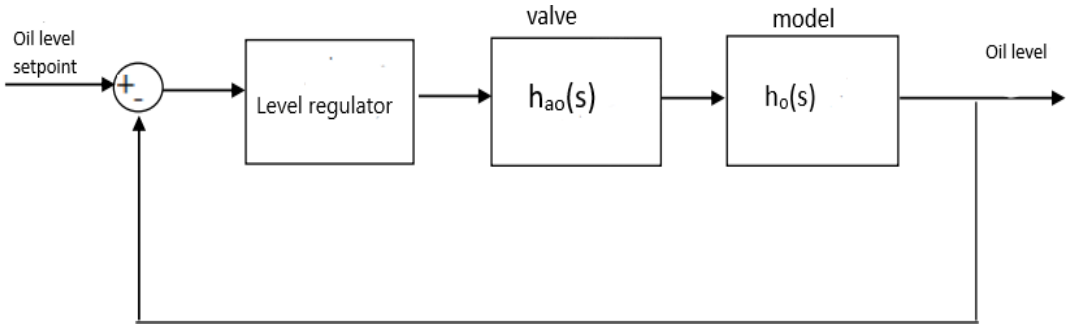

Figure II.7 Oil level control loop.

The transfer function of the oil level control loop is given by:

$$H_o(s) = h_o(s).h_{a_o}(s) \quad \text{II-85}$$

$$H_o(s) = \frac{4{,}037.10^{-3}}{s(6s+1)}.\mathrm{e}^{-5s} \quad \text{II-86}$$

II.5.3 Gas pressure control loop

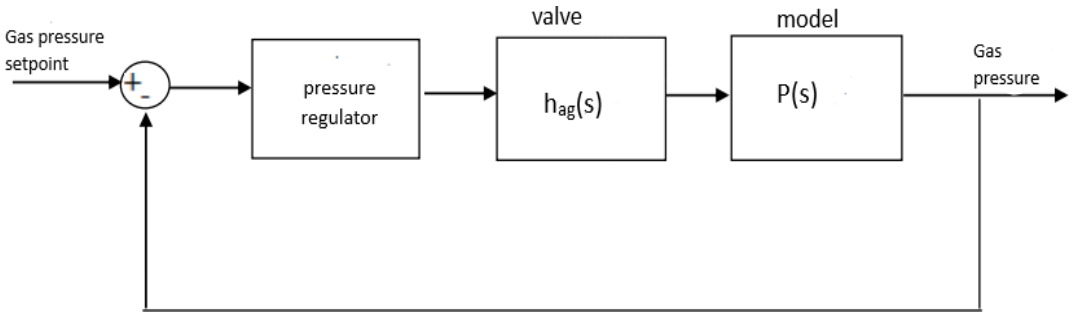

Figure II.8 Gas pressure control loop.

The transfer function of the Gas pressure control loop is given by:

$$P(s) = p_g(s).h_{a_g}(s) \quad \text{II-87}$$

$$P(s) = \frac{120{,}377}{s(6s+1)} \quad \text{II-88}$$

II.6 Process limitations

This section will study the separation process and process control to determine their main limitations because every process has some shortcomings.

II.6.1 Limitations imposed by time delay [10]

Time delay has a substantial impact on control performance, which is mathematically stated in the Equation below II-89. Time lag causes delays in reacting to changes, which slows down the process as a whole. This restriction arises because each change has a waiting period before it can be implemented [13].

$$h(s) = \mathrm{e}^{-cs} \qquad \text{II-89}$$

The block diagram of transport delay within a feedback regulated loop is shown in the Figure II.9 below.

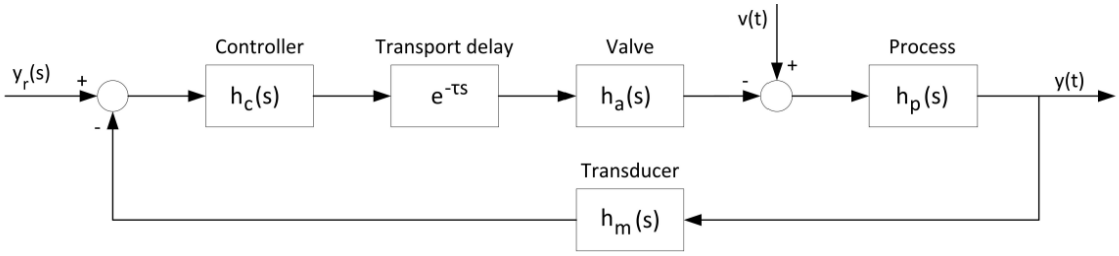

Figure II.9 Block-diagram of a feedback-controlled loop with transport delay.

The phase diagram of the function from the Equation of time delay is plotted in the Figure II.10 below. No matter the frequency, the loop's magnitude, denoted by 0 [dB], stays the same, however the time delay has an impact on the loop's phase. Beyond a certain frequency, it becomes challenging to maintain a phase lead when there is a time delay in the process.

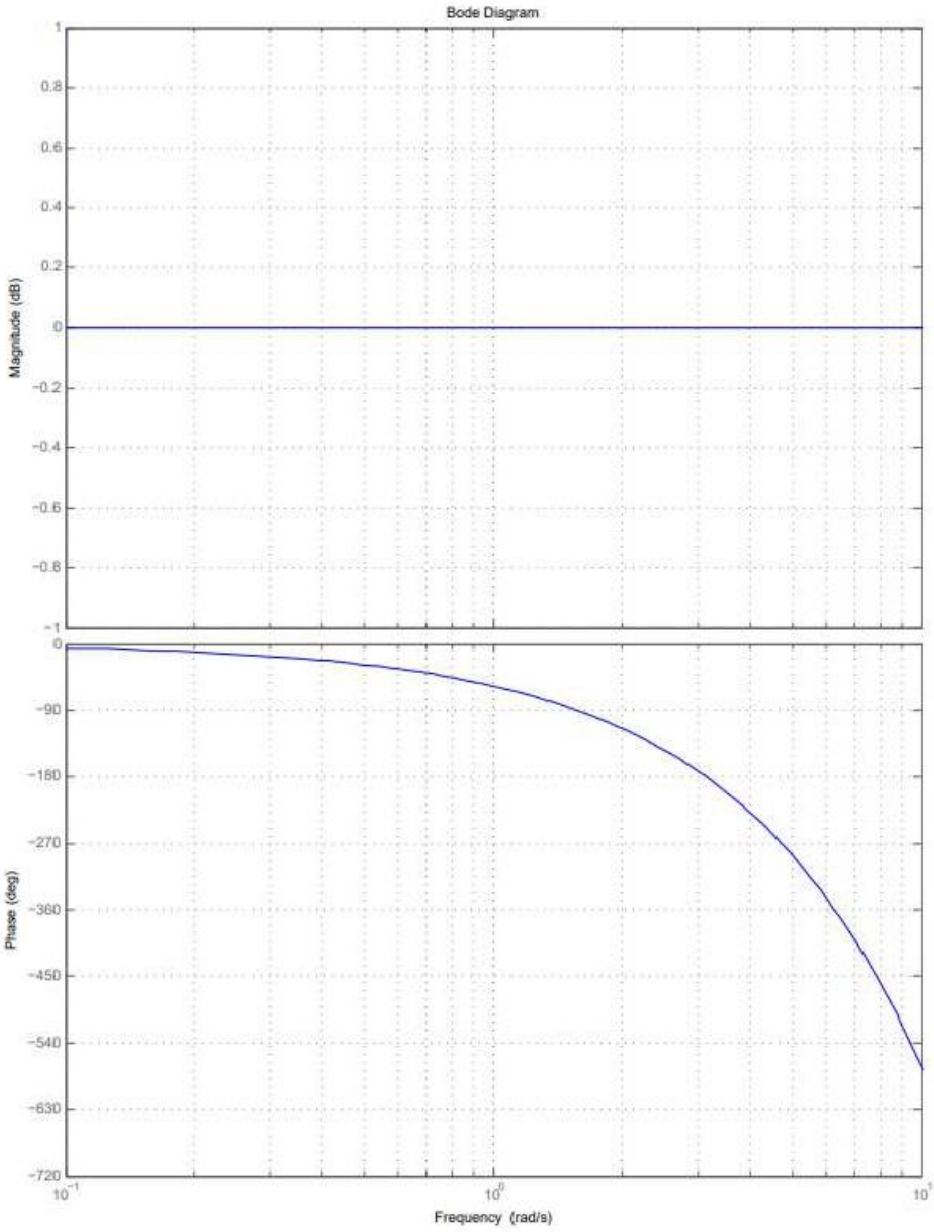

Figure II.10 Bode diagram of the time delay function e $-\tau s$ where $\tau = 1$.

II.6.2 The effect of noise [10]

All actual processes must account for noise, which might have an impact on the process by changing the measurement signal. Noise cannot be completely eliminated, despite efforts to reduce its effects through the use of screens and signal filters. The noise is often a random signal with a zero-mean value, also known as white noise. Band-limited white noise is generally added to the measurement to mimic noise in the separator model [13].

Noise can cause measurement uncertainty, which makes it challenging to precisely calculate the process's real value. The true process value cannot be accurately recognized when noise impact is substantial. Additionally, the actuator may work continually as a result of noise that is amplified by the controller, resulting in mechanical wear and tear. For instance, a globe valve's stem could deteriorate and leak through the packaging.

The controller gain in separator control will be constrained by the presence of noise. Noise is only present in the process measurements for this particular process, and it has been noticed that it will make up 1% of the measurement value. All signals and process outputs must adhere to this maximum 1% peak-to-peak value. As a result, the controller gain will be limited to a maximum value of one without filtering the noise.

Filters like first or second order filters can be used in the control system to lessen the impacts of noise. The performance of the control structure will be constrained by the filter's properties. For instance, a low pass filter might add a new time constant to the system, potentially causing phase lag. In order to achieve the best possible operation of the control system, a well-designed filter must be based on the characteristics of the plant.

II.6.3 Limitations caused by phase lag [10]

Theoretically, there are no essential restrictions placed on phase lag brought on by minimum-phase elements. But in reality, there are frequently certain restrictions that might appear.

The gain will be greatly decreased at high frequencies in the minimum-phase system represented by Equation (II-90), where $|h(\mathrm{j}\omega)| \approx (\frac{\mathrm{k}}{\Pi T_{\mathrm{i}}})\omega^{-n}$. Even when saturation is not a concern, a significant phase lag at high frequencies in the plant, as given by Equation (II-90) taken here for illustration from [12], can be problematic in practice. This is due to the fact that the system must have a positive phase margin for $\omega_c > -180$ degrees in order to be stable. As a result, the system's stability criteria is $\omega_c < \omega_{180}$.

$$h(s) = \frac{\mathrm{k}}{(1+T_1 s)(1+T_2 s)\ldots} = \frac{\mathrm{k}}{M_{\mathrm{i}=1}^{n}(1+T_{\mathrm{i}} s)} \qquad \text{II-90}$$

The stability bounds for proportional (P) or proportional-integral (PI) control are given by $\omega_c < \omega_u$, which is also the practical stability bound for proportional-integral-derivative (PID) control.

The stability bounds for a proportional (P) or a proportional-integral (PI) controller are determined by the imposed phase lag. For a proportional (P) controller, the stability bound is given by $\omega_{180} = \omega_u$, while for a proportional-integral (PI) controller, it is given by $\omega_{180} < \omega_u$. The fundamental limitation on the stability bound for a P or a PI controller is expressed by the Equation $\omega_c < \omega_u$.

It is important to insert zeroes into the controller to give a phase lead in order to increase the gain and crossover frequency c past u. This can be done by employing a derivative action, which cancels out the negative phase that the plant has introduced. At high frequencies, a conventional proportional-integral-derivative (PID) controller may deliver a maximum phase lead of 90 degrees, though in reality it is generally less. The same equation $\omega_c < \omega_u$ provides the practical performance bound for a PID controller.

II.6.4 Limitations due to variable process parameters [10]

Variations in one process variable can have an impact on other process variables in a system because they are frequently interconnected, especially when there are time constants, delays, or quick responses involved. Smaller variation tolerances might be required to keep all process variables within allowable ranges as a result, which can limit the speed of the control performance. To maintain system stability when numerous process variables are interconnected, tighter control of each variable is required.

The plant structure and the physical relationship between the variables govern how nonlinearity is introduced into the system when process variables are coupled. This is covered in this report. It may be essential to handle this by using nonlinear techniques or by linearizing the system around a particular point.

The consequences of dependency between process variables are not always nonlinear. For instance, the level of the upper liquid is linearly dependent on the level of the lower liquid in a tank with straight vertical sides that contains two unmixed liquids. However, as pressure is not linearly related to volume, the gas pressure in a closed tank does not depend on the liquid level.

II.7 Conclusion

Control-oriented modelling of the 10-V-255 three-phase separator is addressed in this chapter. The modelling procedure is based on first-principle laws with the aim to construct simplified models of water level, oil level and gas pressure that can capture the key separator dynamics. Relying on physical laws, we first derived nonlinear models for each of the separator components. Then, in order to make them feasible for separator control loops design, we derived linearized models about the process set-points. From the analysis of the separator dynamics, we noticed the system complexity over the severe nonlinearities and interactions involved. These impose some limitations that we described in the last section. These limitations should be accounted for while dealing for separator control structure design and tuning.

CHAPTER III Separator water level loop control structure design and tuning

III.1 Introduction

In the petroleum industry, the efficient separation of oil, gas, and water is essential for optimizing production and ensuring the quality of extracted resources. Separator control system plays a crucial role in achieving this separation by regulating the flow and levels of each phase within the separator. Actually, the control configuration is built upon advanced instrumentation, control loops, and algorithms to maintain suitable control over the admissible separator operating range. By carefully managing the interface levels, pressure differentials, and flow rates, a reasonable control strategy may ensure effective phase separation, maximize resource recovery, and enhance operational efficiency. This chapter provides a comparative study of different control design methods, including traditional (PID-ZN, PID-SIMC) and intelligent techniques (PID-PSO, RECCo) that have been tested in simulation on the 10-V-255 separator model.

III.2 Robust evolving cloud-based control (RECCo) method

III.2.1 The structure of the RECCo controller

In this section the RECCo controller will be described. The control algorithm consists of three different parts: reference model, evolving law, and adaptation law. All this parts are schematically presented in Figure III.1. Theoretically, the controller could be initialized from the first data sample received. But of course, any existing information about the controlled process can be used to suitably initialize the design parameters. After the initialization, for every incoming sample the controller gains are adapted and, if the certain conditions are satisfied, a new data cloud (fuzzy rule) is added. The Robust Evolving Cloud-based Controller (RECCo) is a type of ANYA fuzzy rule-based system with non-parametric antecedents (IF part). This method applies the concept of fuzzy data clouds and normalized relative data density to define the membership of the current data to the existing clouds. The clouds represent sets of previous data samples which are close to each other. Incoming data samples are analysed in an online manner

and each sample is associated with one of the clouds and only the parameters of that cloud are updated. As we already said, the RECCo controller is based on the ANYA FRB system proposed in [14] and has the following form:

$$R^i : \text{IF } (x \sim X^i) \text{ THEN } (u^i) \qquad \text{III-1}$$

where the number of rules R^i is equal to the number of the clouds in the data space $i = 1. . . c$, and moreover, it changes during the control process. The non-parametric antecedent part is defined with the operator $\sim$ which could be linguistically expressed as 'is associated with' and that means that the current data $x = [x1, x2. . . x_n]^T$ is related to the i^{th} cloud $X^i \in R^n$. The consequent part is defined by c different (partial) control actions u^i for each rule.

RECCo controller can work with different forms of defuzzification such as weighted average, center-of-gravity, "winners takes all" and some mixed forms (e.g. parameterized defuzzification). The degree of association between the data sample x and corresponding cloud X^i is measured by the normalized relative density as follows:

$$\lambda^i_k = \frac{\gamma^i_k}{\sum_{j=1}^{c} \gamma^i_k} \quad i = 1, \dots, c \qquad \text{III-2}$$

where γ^i_k is the local density of the i^{th} cloud for the current data x. The local density calculation in the following subsection will be explained in detail, together with the evolving law of the RECCo controller.

III.2.2 The procedure of the RECCo control algorithm

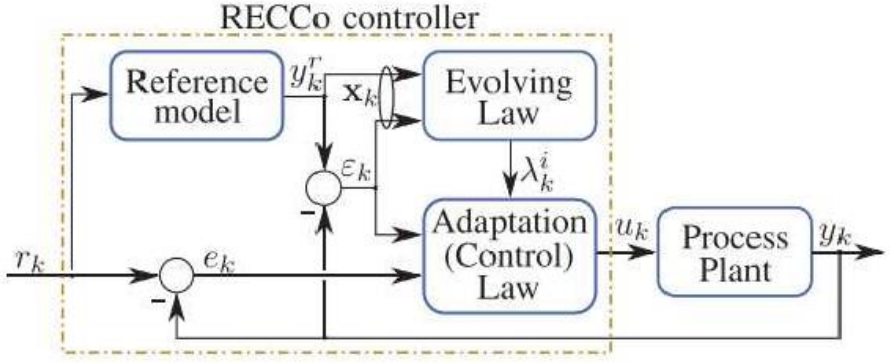

Figure III.1 Control scheme of the RECCo algorithm [16].

III.2.2.1 Reference model

Choosing an appropriate reference model is a very important part of the proposed adaptive system design. General suggestions for selecting the reference model dynamics are that the time constants have to be similar (usually slightly shorter) to those of uncontrolled process. The reference model order would be at less or equal to the order of the plant. Furthermore, the initial conditions of the reference model would then need to have the same values as the initial plant ($y^r_0 = y_0$). The reference model part of the RECCo controller defines the desired trajectory y^r_k and the dynamics that the plant output y_k should follow. In this case we define simple first order linear reference-model as:

$$y^r_{k+1} = a_r y^r_k + (1 - a_r) r_k \qquad 0 < a_r < 1 \qquad \text{III-3}$$

where the parameter a_r is the pole of that model. It can be approximated by (1 − Ts/Tau), where Ts is the sampling period of the process and Tau is the time constant of the reference model which is slightly shorter than the estimated time constant of the controlled plant. In (III-3) the r_k is the reference signal and the y^r_k represents the desired trajectory of the plant output y_k. The goal of the controller is to provide efficient performance and to ensure that the tracking error:

$$s_k = y^r_k - y_k \qquad \text{III-4}$$

is as small as possible (in the presence of disturbances and modelling errors). When dealing with adaptive and evolving (online learning) systems we need to construct reference with changing steps in some operating range [r_{min}, r_{max}]. In this case the user (operator) of the process only chooses the limit values r_{min} and r_{max} and the RECCo algorithm constructs the step changes in this interval. We have to note here that the RECCo controller is not limited only to this type of reference model (first order linear model), but also other types could be used according to the dynamics of the controlled process.

III.2.2.2 Evolving law

The evolving law in this paper consists only a mechanism for adding new clouds (rules). Beside this, another evolving mechanisms such as merging, splitting and removing clouds can be also implemented. We use just adding mechanism due to simplicity of the implementation and because it is sufficient for the control of the plant investigated here. The adding mechanism relies on the local density γ_k of the current data sample with the existing clouds. The local density

takes into consideration all the data samples from one particular cloud (therefore local) and is calculated using a suitable kernel K:

$$\gamma^{i}_{k} = \kappa\left(\sum_{j=1}^{M^{i}} d^{i}_{k_j}\right) \quad \text{III-5}$$

where M_i is the number of data samples in i^{th} cloud and $d^{i}_{k_j}$ is the distance between the current data sample x_k and the j^{th} sample x^{i}_{j} from the i^{th} cloud. In all the equations the superscript in variables (e.g. i in x^{i}_{k}) refers to the clouds, while the subscript refers to the time stamp (e.g. k in x^{i}_{k}). As we can see in (III-5) this approach directly takes into account all previous data samples. Using a Cauchy kernel as was proposed in [15], the local density of the i^{th} cloud is defined as follows:

$$\gamma^{i}_{k} = \frac{1}{1+\frac{\sum_{j=1}^{M^{i}} (d^{i}_{k_j})^2}{M^{i}}} \quad \text{III-6}$$

where $\sum_{j=1}^{M^{i}} (d^{i}_{k_j})^2$ is the sum of the square of Euclidean distances ($d^{i}_{k_j} = \|x_k - x^{i}_{j}\|^2$) between the new data x_k and all data points of the i^{th} cloud. For easier practical and computational implementation, local density (III-6) can be recursively rewritten as follows:

$$\gamma^{i}_{k} = \frac{1}{1+\|x_k - \mu^{i}_{k}\|^2 + \sigma^{i}_{k} - \|\mu^{i}_{k}\|^2} \quad \text{III-7}$$

where μ^{i}_{k} is the mean value of the cloud's data is points and σ^{i}_{k} is the mean-square length of the data vectors in the ith cloud. Both of them can be recursively calculated using following equations for mean value and mean-square length, respectively:

$$\mu^{i}_{k} = \frac{M^{i}-1}{M^{i}} \mu^{i}_{k-1} + \frac{1}{M^{i}} x_k \quad \text{III-8}$$

$$\sigma^{i}_{k} = \frac{M^{i}-1}{M^{i}} \sigma^{i}_{k-1} + \frac{1}{M^{i}} \|x_k\|^2 \quad \text{III-9}$$

The evolving law consists the mechanism of adding new clouds and is the same as the one presented in [16]. Once a new data sample arrives, we need to calculate c different local densities between the sample and all the existing clouds. According to the maximal local density, the data sample is associated with that cloud and furthermore, the parameters of that cloud are updated using Eqs. (III-8) and (III-9). Theoretically, it is possible to happen that the current data

sample has the same density to two or more clouds. In that case we associate that data sample with the oldest cloud (the one that was added before the others). But, if the maximal local density is lower than the threshold value max (the current data sample is far away from all existing clouds), a new cloud is added. The cloud's data space is normalized, and due to this the default value of the threshold can be fixed γmax = 0.94. Some conservatism is always welcome when changing the structure of the evolving system. This is why some other criteria need to be fulfilled before adding a new cloud (such as certain time n_{add} has passed from the last change). We have to note that in our current case study we use the value of this parameter n_{add} = 40. We can summarize the whole evolving procedure presented above in the pseudo Algorithm 1 (see lines from 9 to 22) Figure III.2.

Algorithm 1. Pseudo code of the RECCo PID control algorithm.

1: Initialize (Process parameters): τ, T_s, u_{min}, u_{max}, r_{min}, r_{max}.
2: Initialize (Evolving parameters): γ_{max}, $c = 0$, c_{max}, n_{add}.
3: Initialize (Adaptation parameters): α_P, α_I, α_D, α_R, σ_L, d_{dead}, $\underline{\theta}$, $\overline{\theta}$.
4: **repeat**
5: Measurement: y_k.
6: Define and compute: y_k^r ▷ *Reference model*
7: Compute: e_k, ε_k, Σ_k^{ε}, Δ_k^{ε}.
8: Compute: $\mathbf{x}_k = [\ \varepsilon_k/\Delta\varepsilon,\ (y_k^r - r_{min})/\Delta r\ ]^T$.
9: **if** $c = 0$ **then** ▷ *Start of the evolving law*
10: Increment: c,
11: Store: k_{add},
12: Initialize: μ_0^1, σ_0^1, θ_0^1.
13: **else**
14: Calculate: γ_k^i, λ_k^i, where $i = 1, \ldots, c$
15: **if** $(max_i\gamma_k^i < \gamma_{max}$ **and** $k > (k_{add} + n_{add}))$ **then**
16: Increment: c,
17: Store: k_{add},
18: Initialize: μ_0^c, σ_0^c, θ_0^c.
19: **else**
20: Associate sample $\mathbf{x}_k$ with cloud $(max_i\gamma_k^i)$
21: Update μ_k^i, σ_k^i for the cloud $(max_i\gamma_k^i)$
22: **end if**
23: **end if** ▷ *End of the evolving law*
24: Adaptation of the **PID controller gains**.
25: Computation of the **control law**.
26: **until** End of data stream.

Figure III.2 Pseudo-code of the RECCo controller algorithm [16].

III.2.2.3 Adaptation law

For the consequent part of the RECCo controller the PID-type control is used [16] and each cloud (fuzzy rule) has its own PID parameters. The vector of the parameters is denoted as $\theta^{i}_{k} = [P^{i}_{k}, I^{i}_{k}, D^{i}_{k}, R^{i}_{k}]^{T}$ and parameters ofthe first cloud are initialized with zeros $\theta^{1}_{0} = [0,0,0,0]^{T}$, while all later added clouds are initialized with mean value of the parameters of all previous clouds as follows:

$$\theta^{C}_{0} = \frac{1}{c-1}\sum_{j=1}^{c-1} \theta^{i}_{k} \qquad \text{III-10}$$

where c is the index of the newly added cloud. After the classification of the current data sample to one of the clouds, only the PID parameters of that cloud are adapted while the parameters of other clouds are kept constant:

$$\theta^{i}_{k} = \theta^{i}_{k-1} + \Delta\theta^{i}_{k} \qquad \text{III-11}$$

And the adaptation of the PID parameters is achieved as follows [28]:

$$\Delta P^{i}_{k} = \alpha_{p} G_{sign} \lambda^{i}_{k} \frac{|e_k s_k|}{1+r_k^2} \qquad \text{III-12}$$

$$\Delta I^{i}_{k} = \alpha_{I} G_{sign} \lambda^{i}_{k} \frac{|e_k \Delta^{s}_{k}|}{1+r_k^2} \qquad \text{III-13}$$

$$\Delta D^{i}_{k} = \alpha_{D} G_{sign} \lambda^{i}_{k} \frac{|e_k \Delta^{s}_{k}|}{1+r_k^2} \qquad \text{III-14}$$

$$\Delta R^{i}_{k} = \alpha_{R} G_{sign} \lambda^{i}_{k} \frac{s_k}{1+r_k^2} \qquad \text{III-15}$$

where α_p α_I α_D α_R are the adaptation gains of the controller parameters, $G_{sign} = \pm 1$ is the known process gain sign, λ^{i}_{k} is the normalized local density of the cloud, ε_k is the tracking error while the control error is denoted as ek = rk − yk. The discrete-time derivative is denoted as ε_k and will be discussed later. In (III-12 to III-15) only the adaptation gains should be set initially. The default value of the parameters is 0.1 and is used when the range of the control variable is (umin = 0/4, umax = 20). When the range is different, the value of the parameters is scaled as follows:

$$\alpha_{new} = \frac{umax-umin}{20} * 0.1 \qquad \text{III-16}$$

But in our case we used a different scale to ensure the best response:

$$\alpha_{new} = \frac{umax-umin}{0.15} * 0.01 \qquad \text{III-17}$$

For a PID-type controller, the rule consequent has the following form:

$$u^i_k = P^i_k s_k + I^i_k \sum^s_k + D^i_k \Delta^s_k + R^i_k \qquad \text{III-18}$$

where P^i_k I^i_k D^i_k arw controller gains while R^i_k is compensation of the operating point. While the adaptation of the parameter R^i_k in (III-12 to III-15) is driven only by tracking error εk this parameter tries to correct the offset error of the current operating point. Discrete-time integral and derivative of the tracking error, respectively, are calculated as follows:

$$\sum^s_k = \sum_{k=0}^{k-1} s_k = \sum_{k-1} + s_{k-1} \qquad \text{III-19}$$

$$\Delta^s_k = s_k - s_{k-1} \qquad \text{III-20}$$

Finally, for the defuzzification the weighted average is used and furthermore, the control variable becomes:

$$u_k = u_{min} + \sum_{i=1}^{c} \lambda^i_k u^i = u_{min} + \frac{\sum_{i=1}^{c} {}^i_k u^i}{\sum_{i=1}^{c} {}^i_k} \qquad \text{III-21}$$

where u^i denotes the ith (partial) rule consequent and normalized relative density (III-2) is used.

III.2.5 Application to water level control loop

The response of the water level control loop obtained with the robust evolving cloud based control (RECCo) method is presented in Fig. III. This result is based on the parameter settings shown in the figure below. It turns out the following performance indices:

Response time: 110s

Rise time: 45s

Overshoot: 10%

```
%%% Evolving Parameters Initialization %%%
nN = 20; % Must check : Cntrl + H
gammaMx = 0.94; %0.93
nadd = 40; % 20
%%% Process Parameters Initialization %%%
umax = 150; %
umin = 0; % Must check : Cntrl + H
rmax = 1; % Must check r(k) in the model AND in the main .m file
rmin = 0; % Must check r(k) in the model AND in the main .m file
dltar = rmax-rmin;
dpslnk = dltar/2;
%%% Adaptation Parameters Initialization %%%
dead = 0.29; %
Max = 0.15; % Default value is 20
cnstP = (((umax-umin)/Max)*10); %
cnstI = (((umax-umin)/Max)*0.01); %
cnstD = (((umax-umin)/Max)*0.01); %
cnstR = (((umax-umin)/Max)*0.01); %
sigP = 0.2; %
sigI = 0.01; %
sigD = 0.01; %
sigR = 0.01; %
```

Figure III.3 The control parameters of the RECCo used in the Matlab simulation.

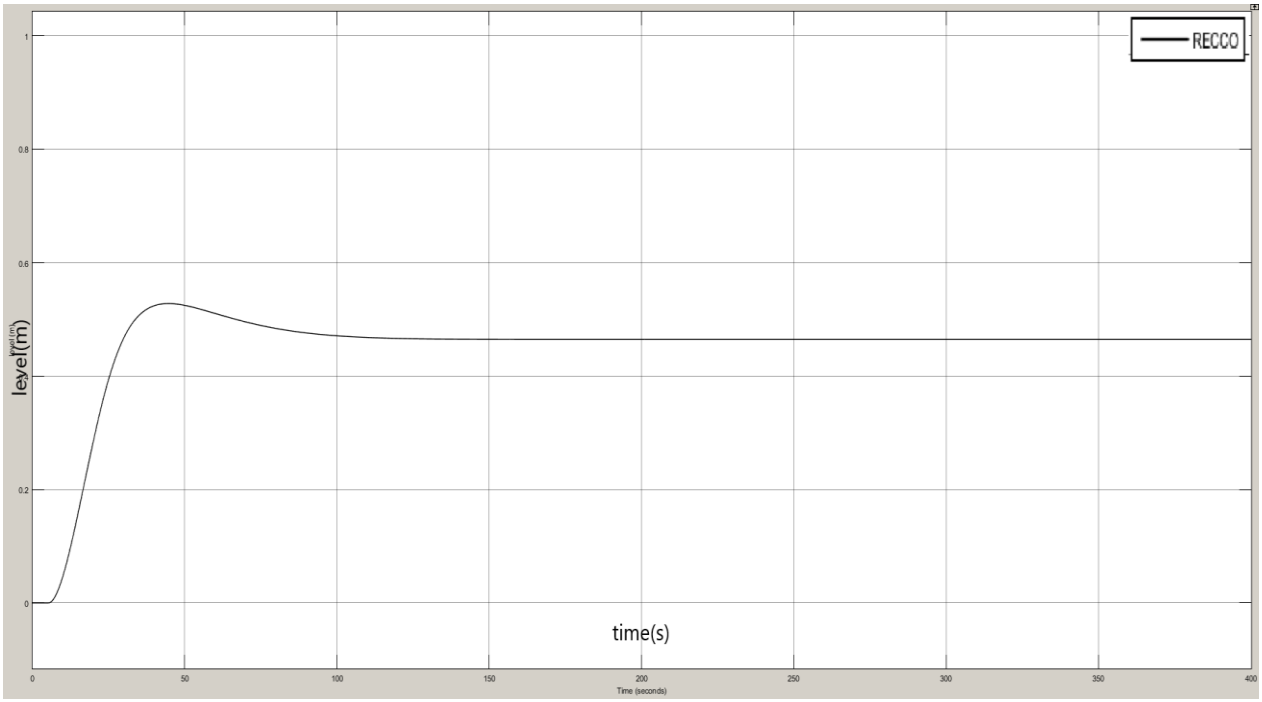

Figure III.4 Water level response under RECCo control.

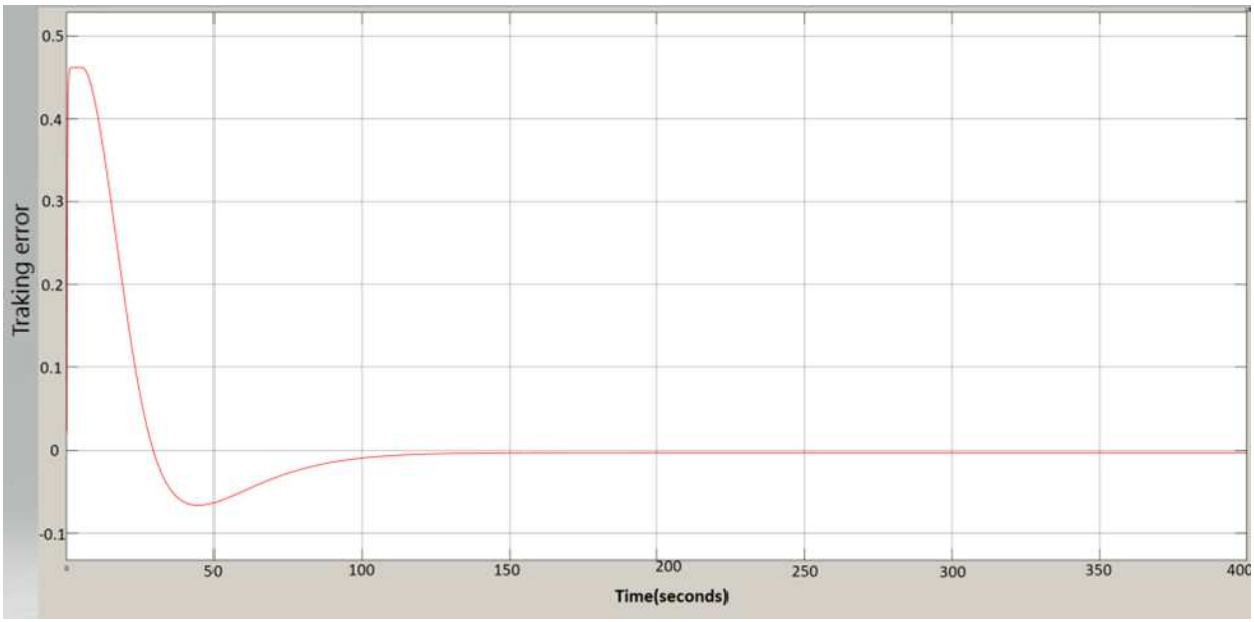

Figure III.5 The tracking error obtained under RECCo control.

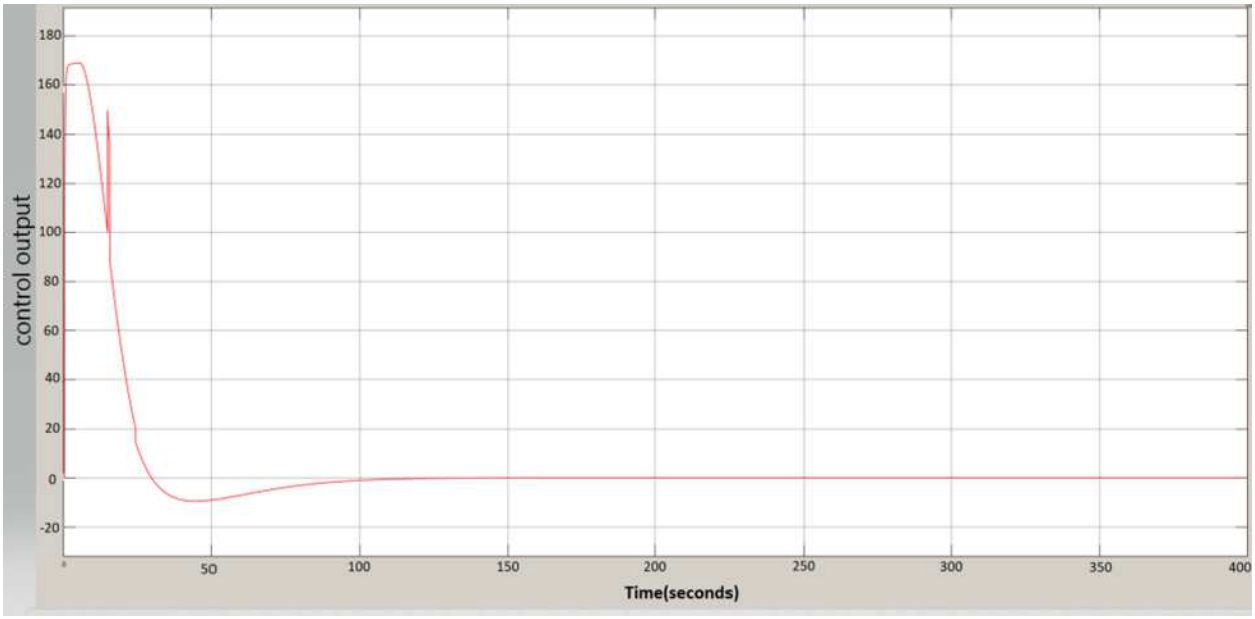

Figure III.6 The RECCo control output.

III.3 Conventional Ziegler-Nichols control method

The Ziegler-Nichols method is a popular method for tuning P, PI, and PID controllers. It starts by zeroing the integral and differential gains and then raising the proportional gain until the

system is unstable. The Ziegler-Nichols closed-loop tuning method allows us to use the ultimate gain value, K_{cr}, and the ultimate period of oscillation, Pu, to calculate K_p. It is a simple method of tuning PID controllers and can be refined to give better approximations of the controller.

The controller is in automatic mode with a low value of K_p. The integral and derivative actions are inhibited by setting $T_i = 0$ and $T_d = 0$.

The gain K_p of the proportional controller acting alone is gradually increased until the desired loop oscillation (loop pumping) is achieved [18].

The ultimate gain (K_{cr}) leading to loop pumping and the period of oscillations (T_{cr}) corresponding to this operation are determined from any observation point (controller output, process output, etc.).

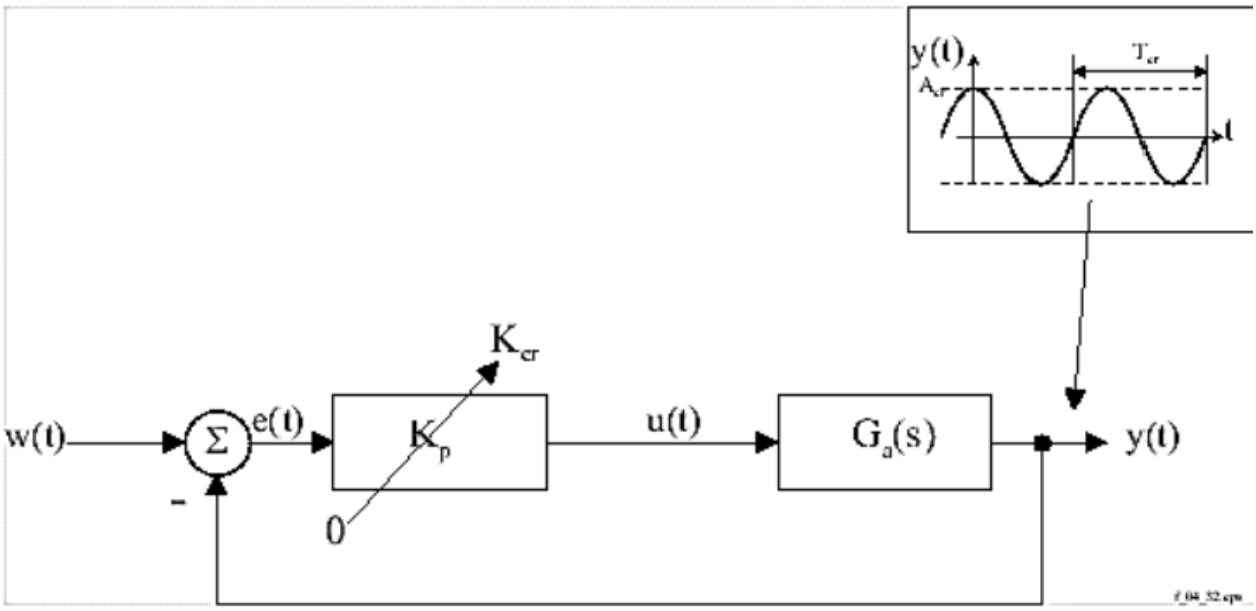

Figure III.7 Oscillation of a system with a proportional controller [17].

Ziegler & Nichols proposed to calculate the parameters of the chosen controller using the following rules:

Controller	K_P	T_i	T_d
P: $R(s) = K_P$	$0.5K_{cr}$	*	*
PI: $R(s) = K_P(1 + \frac{1}{s*T_\mathrm{i}})$	$0.45K_{cr}$	$0.835T_{cr}$	*
PID: $R(s) = K_P(1 + \frac{1}{s*T_\mathrm{i}} + T_d * s)$	$0.6K_{cr}$	$0.5T_{cr}$	$0.1255T_{cr}$

Table III-1 Ziegler-Nichols tuning rules of PID parameters [18].

III.3.1 Application to water level control loop

The transfer function of the loop is:

$$H_\mathrm{w}(s) = \frac{1{,}936.10^{-4}}{s(6s+1)} . \mathrm{e}^{-5s} \qquad \text{III-22}$$

Figure III.3 shows the response of the closed-loop system with a propo tional controller, after gradually increasing the gain Kp until obtaining oscillations (pumping) for Kcr = 1144.

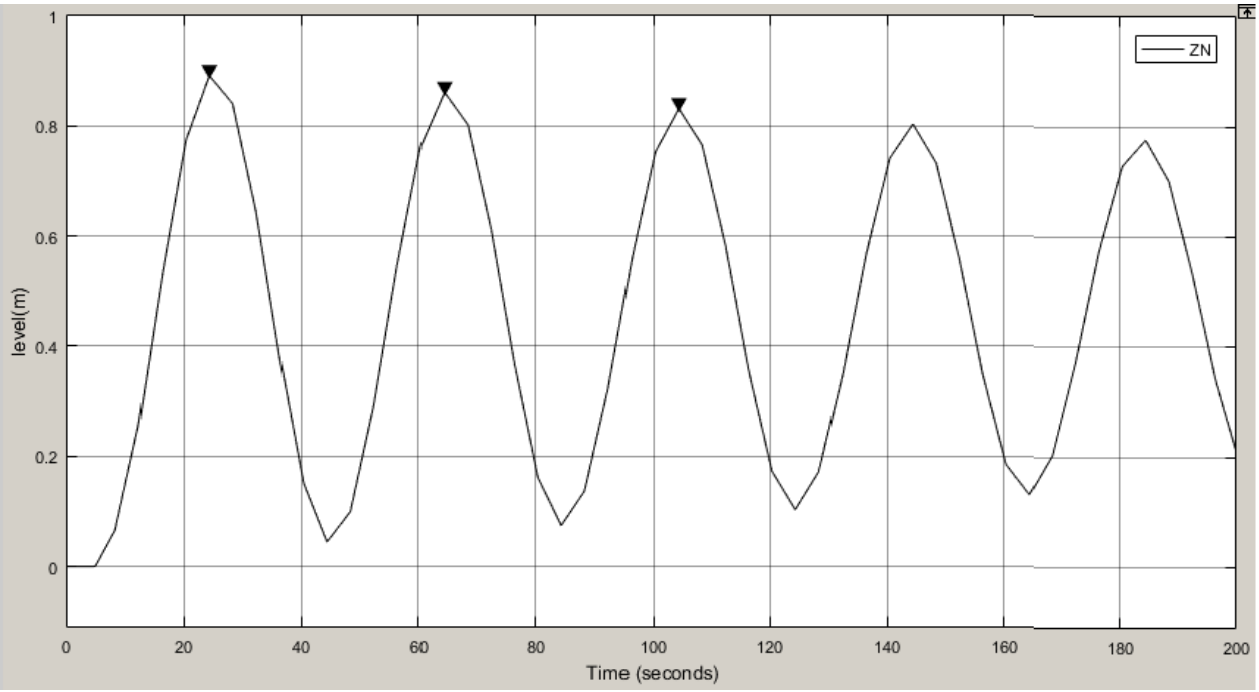

Figure III.8 Response of the closed-loop system with a proportional controller at critical gain.

According to Figure III.8, we have T_{cr} = 40s. Using Table III.1, we found:

$k_P = 0.6K_{cr}$ $k_P = 686{,}4$

$T_i = 0.5T_{cr}$ $T_i = 20s$

$T_d = 0.125T_{cr}$ $T_d = 5s$

III.4 Internal model-based (SIMC) control method

The SIMC (Skogestad's Internal Model Control) method is a two-step procedure for smooth PID controller tuning. The first step of the SIMC procedure is to obtain a first- or second-order plus delay model. The second step is to derive model-based controller settings. PI-settings result if we start from a first-order model, whereas PID-settings result from a second-order model. The SIMC method has already found widespread industrial usage and has been shown to work well on a wide range of processes [17].

III.4.1 Derivation of the SIMC tuning rules

As mentioned above, we first need to obtain a second-order plus dead-time (SOPDT):

$$G(s) = \frac{k}{(c_1 s+1)(c_2 s+1)} e^{-\theta s} \quad \text{III-23}$$

where k is the process gain, θ is the dead-time, and τ_1 and τ_2 are the time constants [19].

Then we determine the desired closed-loop time constant (τ_c) which specifies the desired performance of the system response.

For a PID controller, the transfer function is:

$$C(s) = K_P \left(1 + \frac{1}{s * T_i} + T_d * s\right) \quad \text{III-24}$$

The closed-loop transfer function is:

$$\frac{y}{y_s} = \frac{G(s).C(s)}{G(s).C(s)+1} \quad \text{III-25}$$

The output y is considered undisturbed, the idea of direct synthesis is to specify the desired transfer function in closed-loop and solve the system to obtain the controller parameters. Thus, we can write:

$$C(s) = \frac{1}{G(s)} . \frac{1}{\frac{1}{(y/y)_{s_{desired}}} - 1} \qquad \text{III-26}$$

The desired transfer function is considered as a first order with a dead-time θ and a time constant τ_c given in the form

$$\left(\frac{y}{y_s}\right)_{desired} = \frac{1}{c_c s + 1} e^{-\theta s} \qquad \text{III-27}$$

Replacing III-27 in III-26 gives:

$$C(s) = \frac{(c_1 s+1)(c_2 s+1)}{k} \frac{1}{c_c s + 1 - e^{-\theta s}} \qquad \text{III-28}$$

The approximation of delay using the first-order Taylor series expansion allows us to write $e^{-\theta s} \approx 1 - \theta s$, this will give us:

$$C(s) = \frac{(c_1 s+1)(c_2 s+1)}{k} \frac{1}{(c_c+\theta)s} \qquad \text{III-29}$$

The following parameters are the result of the identification of equation III-29 with equation III-28:

$$k_c = \frac{1}{k} . \frac{c1}{c_c+\theta} = \frac{1}{k^F} . \frac{c_1}{c_1+\theta} \qquad \text{III-30}$$

$$\frac{r_1}{k} = k'$$

$$r_I = r_1$$

$$r_d = r_2$$

III.4.2 Modification of the integration constant r_I [19]

Let G(s) be a transfer function of a first-order system with delay:

$$G(s) = \frac{1}{c_c s+1} \mathrm{e}^{-\theta s} \approx k. \frac{1}{c_1 s+1} \approx \frac{1}{c_1 s} \approx \frac{\mathrm{k}^F}{s} \qquad \text{III-31}$$

The characteristic equation of the closed-loop system associating a PI controller and the system G(s) is as follows:

$$\frac{c_1}{\mathrm{k}_c.\mathrm{k}^F} s^2 + r_1 s + 1 = 0 \qquad \text{III-32}$$

The canonical form of the characteristic equation expressed in terms of damping factor and natural frequency is:

$$\mathrm{w}_0^2. s^2 + 2\mathrm{w}_0 \zeta s + 1 = 0 \qquad \text{III-33}$$

By identifying equations III-32 and III-33, we find:

$$\mathrm{w}_0 = \sqrt{\frac{c_1}{\mathrm{k}_c.\mathrm{k}^F}} \qquad \text{III-34}$$

$$\zeta = \frac{1}{2} \sqrt{r_1. k_c. k'} \qquad \text{III-35}$$

The recommended value for a robust system is $\zeta = 1$ [17], this yields:

$$r_1 = 4(r_c + \theta)$$

$$k_c = \frac{1}{k'} . \frac{r_1}{r_1 + \theta}$$

$$r_d = r_2$$

The tuning parameters for a PID/PI controller based on the process type are presented in Table III.2. The other calculation cases listed in the table are specific cases established for G (s) with $r_1 = 0$ or $r_2 = 0$.

Process	G(s)	k_c	r_i	r_d
First order with dead time	$k\frac{e^{-\theta s}}{(r_1 s+1)}$	$\frac{1}{k}\frac{r_1}{r_c+\theta}$	$min\{r_1, 4(r_c+\theta)\}$	-
Second order with dead time	$k\frac{e^{-\theta s}}{(r_1 s+1)(r_2 s+1)}$	$\frac{1}{k}\frac{r_1}{r_c+\theta}$	$min\{r_1, 4(r_c+\theta)\}$	r_2
Dead time	$ke^{-\theta s}$	0	0	-
integrator	$k'\frac{e^{-\theta s}}{s}$	$\frac{1}{k'}\frac{1}{(r_c+\theta)}$	$4(r_c+\theta)$	-
First order with integrator	$k'\frac{e^{-\theta s}}{s(r_2 s+1)}$	$\frac{1}{k'}\frac{1}{(r_c+\theta)}$	$4(r_c+\theta)$	r_2
Double integrator	$k"\frac{e^{-\theta s}}{s^2}$	$\frac{1}{k"}\frac{1}{4(r_c+\theta)}$	$4(r_c+\theta)$	r_2

Table III-2 Tuning parameters for a PID/PI controller using the SIMC method [19].

III.4.3 Determination of the parameter $_c$

The closed-loop time constant (τc) should be set to proper value as to achieve good performance of the system response in closed loop. It should be selected according to the following considerations [19]:

- A smaller τc will result in a faster response, but may cause more overshoot. This is suitable for processes that require fast disturbance rejection.
- A larger τc will result in a slower response, but with less overshoot. This is suitable for stable processes where a slower, smoother response is desired.

III.4.4 Application to water level control loop

The transfer function of the loop is:

$$H_{\mathrm{w}}(s) = \frac{1{,}936.10^{-4}}{s(6s+1)}.\,\mathrm{e}^{-5s} \qquad \text{III-36}$$

It is given in the form:

$$H_{\mathrm{w}}(s) = \frac{\mathrm{k}^{F}}{s(c_2 s+1)}.\,\mathrm{e}^{-\theta s} \qquad \text{III-37}$$

with:

$$r_2 = 6$$

$$\theta = 5$$

$$\mathrm{k}' = 1{,}936.10^{-4}$$

The calculation of kc, Ti, Td, using Table III.2 yields:

$$k_c = \frac{1}{k'}\frac{1}{(r_c+\theta)}$$

$$T_{\mathrm{i}} = 4(r_c+\theta)$$

$$T_d = r_2$$

Table III.3 presents the values of $\mathrm{k_c}$, $\mathrm{T_i}$, and $\mathrm{T_d}$ calculated as a function of τ_{c}.

r_c	k_p	T_{i}	T_d
$r_c = 2.5$	688.7	30	6
$r_c = 5$	516.52	40	6
$r_c = 7.5$	413	50	6

Table III-3 PID controller parameters for the water level loop calculated as a function of r_c

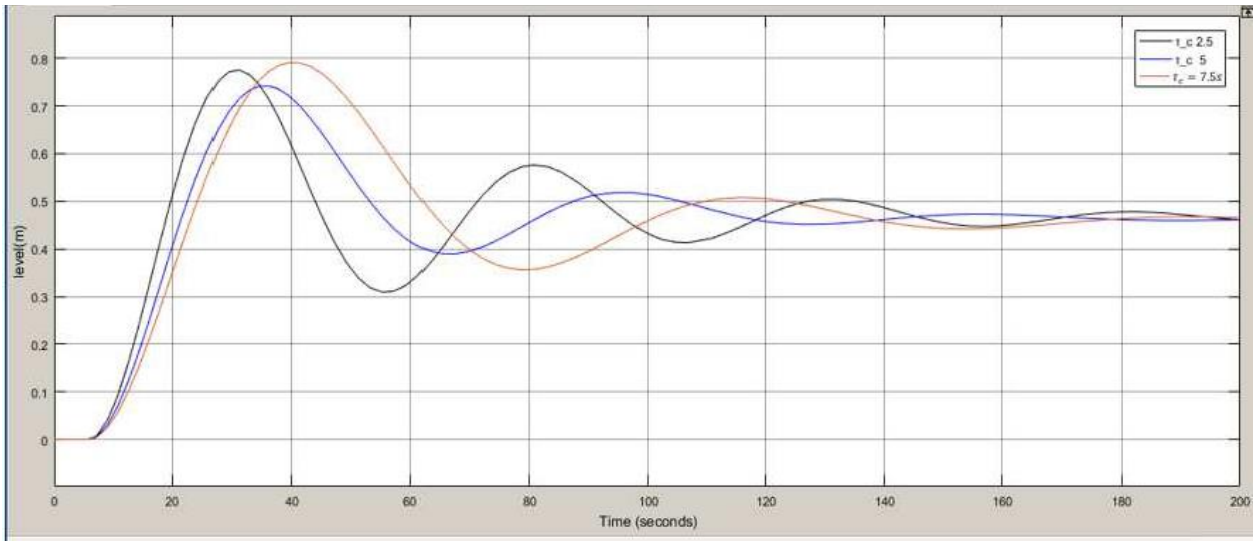

Figure III.9 Water level response for different values of the parameter r_c.

According to the simulation results presented in Figure III.9, for three different values of τ_c, the following observations can be made:

r_c= 2.5 results in an overshoot of 63%

r_c = 5 results in an overshoot of 52%

r_c= 7.5 results in an overshoot of 71%

To achieve a good balance between speed, overshoot, and disturbance rejection, r_c = 5 is chosen for the remaining simulation. This allows us to determine the following parameters for the PID-SIMC controller:

k_c = 516,52

T_i == 40s

T_d = 6s

III.5 Particle Swarm Optimization based control method

Particle Swarm Optimization is a population-based optimization algorithm inspired by the collective behavior of bird flocking or fish schooling [20]. It is commonly used to solve optimization problems where the goal is to find the optimal solution in a search space.

In PSO, a population of particles represents potential solutions to the problem. Each particle moves through the search space and adjusts its position based on its own experience and the experience of neighboring particles. The movement of particles is guided by their individual best-known position (pbest) and the global best-known position (gbest) within the swarm [20].

During each iteration, the particles update their velocities based on two main components: cognitive component and social component. The cognitive component drives the particle towards its personal best position, while the social component guides the particle towards the global best position. These components are weighted by acceleration coefficients, determining the influence of personal and social knowledge on the particle's movement.

By continuously updating their positions and velocities, particles move towards promising regions in the search space. The algorithm iterates until a termination condition is met, such as reaching a maximum number of iterations or achieving a satisfactory solution.

PSO is known for its simplicity and ability to handle both continuous and discrete optimization problems. It has been applied to various domains, including engineering, finance, data mining, and machine learning. PSO's effectiveness lies in its ability to efficiently explore the search space, balancing exploration and exploitation to find optimal or near-optimal solutions [20].

III.5.1 PSO algorithm [20]

This simple algorithmic representation can be used as a reference to understand the flow and steps involved in the PSO algorithm:

1. Initialize the swarm with random particle positions and velocities.

2. Evaluate the fitness of each particle.

3. Set the personal best position (pbest) of each particle to its current position.

4. Set the global best position (gbest) to the position of the particle with the best fitness.

5. While the termination condition is not met:

6. For each particle in the swarm:

7. Update the velocity of the particle based on its current velocity, pbest, and gbest.

8. Update the position of the particle based on its current position and velocity.

9. Evaluate the fitness of the particle's new position.

10. If the new position is better than the particle's pbest, update its pbest.

11. If the new position is better than the gbest, update gbest.

12. Return the best solution found (gbest).

The velocity and the next position of each particle in the swarm is calculated using these equations:

$$v(t) = \mathrm{w}.v(t-1) + c.rand(xp - x(t-1)) + c.rand(xg - x(t-1)) \quad \text{III-38}$$

$$x(t) = x(t-1) + v(t) \quad \text{III-39}$$

III.5.2 Application to water level control loop

The algorithm implementation for tuning PID parameters can be better explained with these simple steps:

- First, we start by creating a Simulink model for the water level control loop (in our case 'normalppl.slx') and then we integrate it into our Matlab code.

- Now we need to set the lower and upper bounds for the PID parameters P, I nd D; the bigger the range the more time it takes for the particles to navigate in the entire range. We finally set the search bounds to:

```
lb = [0.1 0.1 0.1]; % Lower bound
ub = [1000 1000 1000]; % Upper bound
```

- The last thing to do is to set the number of iterations and particles, the higher the value of these two control parameters the more precise the search will be but it will take more computational effort and time:

```
iterations = 15; % No. of iterations

populationSize =15; % No. of particles
```

- Applying the PSO algorithm to tuning the water level PID controller parameters gives the following results:

K_p = 520.63

T_i = 1s

T_d = 1000s

III.6 Control results

The most common control loop is presented in this figure:

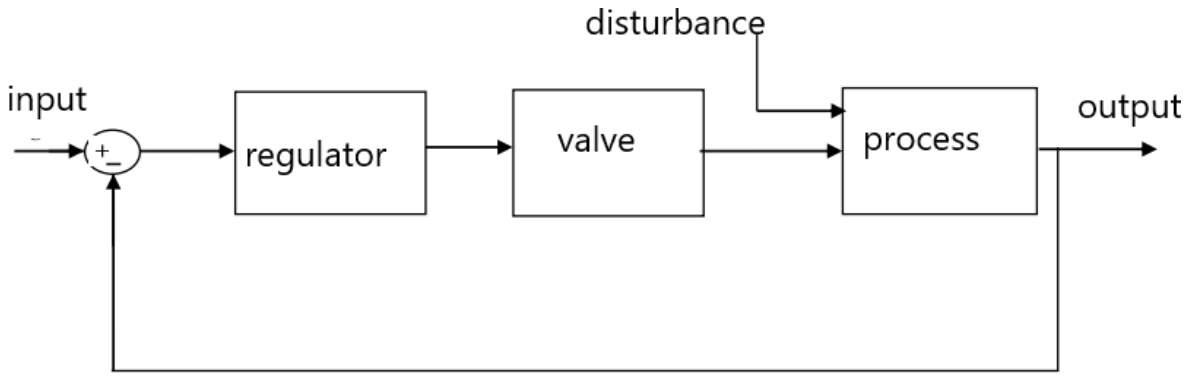

Figure III.10 Typical level control loop for the 10-V-255 separator.

In this section, we proceed with the simulation of the control loop (level) using the results of PID tuning obtained by means of the different design methods described above. We also examine their performance in the presence of slugging, which is one of the most complex phenomena encountered in the treatment separators of hydrocarbon mixtures extracted from oil wells. The slugging phenomenon, which governs the flow in the three-phase separator, is assimilated to a sudden and severe variation introduced at the inlet flow rate.

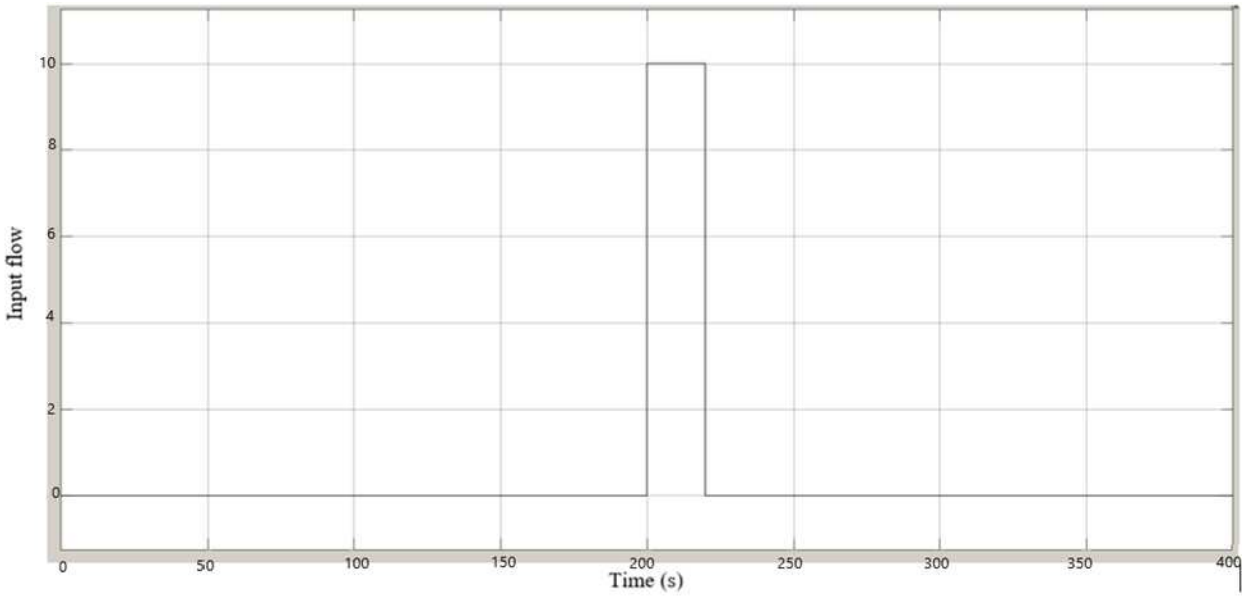

Figure III.11 Representation of the disturbance caused by slugging effect.

III.6.1 Level reference tracking results

The responses of the water level control loop obtained for the different tuning methods are presented and compared in the Figure III.12 below.

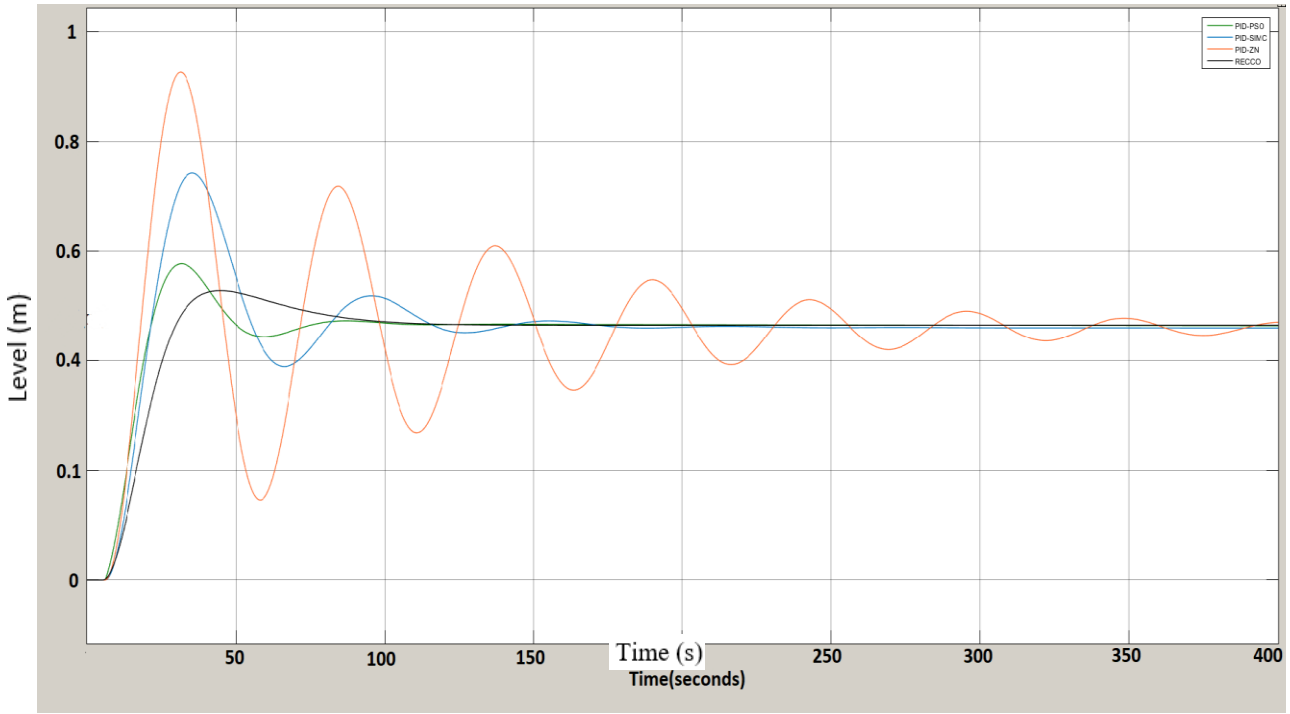

Figure III.12 Water level response under different control strategies.

Tuning method	Response time	rise time	Overshoot
PID-ZN	420s	32s	100
PID-SIMC	190s	35s	52%
PID-PSO	90s	34s	24%
RECCO	110s	45s	10%

Table III-4 Performance of synthesis methods for the water level control loop in the separator 10-V-255 in case of reference tracking

The comparative Table III.4 and the Figure III.12 show and confirm the superiority of the RECCo tuning method compared to ZN, SIMC and PSO methods with the least amount of overshoot.

III.6.2 Slugging effect compensation results

The response of the simulated control loop in the presence of severe disturbance associated with slugging, using different control tuning methods, are illustrated in Figure III.13.

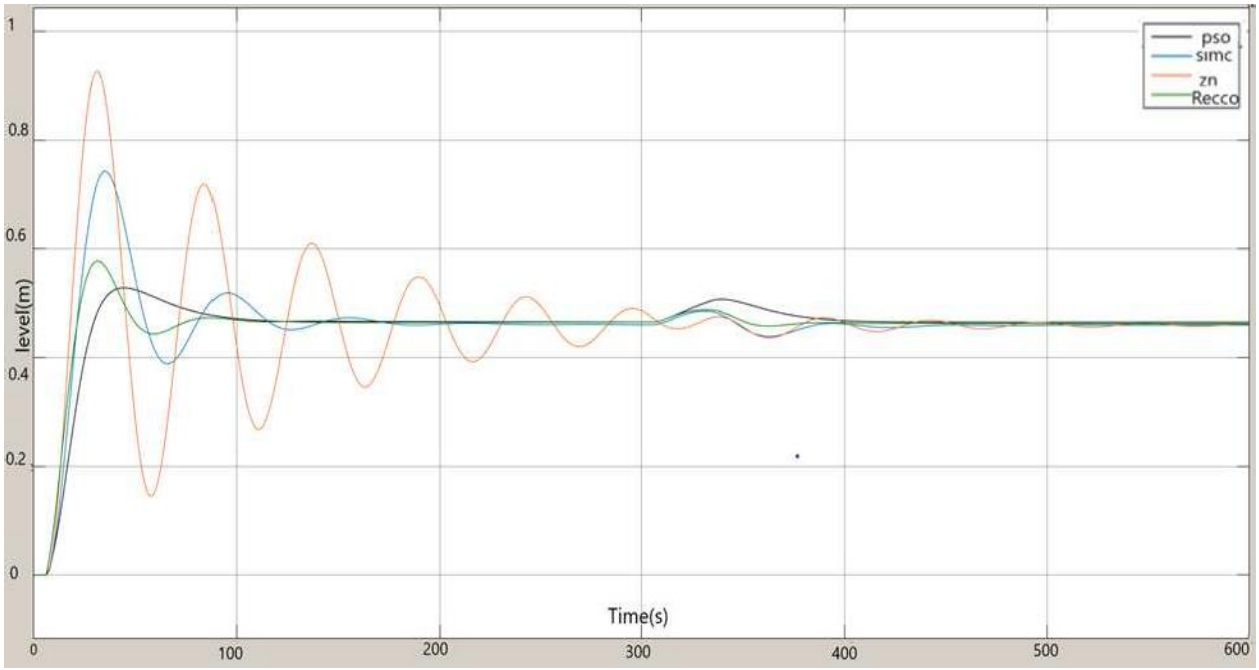

Figure III.13 The water level control loop response with different tuning methods in the presence of slugging.

Tuning method	Disturbance compensation time	Overshoot
PID-ZN	190s	1%
PID-SIMC	150s	2%
PID-PSO	100s	3%
RECCO	80s	10%

Table III-5 Compared performance of different water level loop control methods in case of slugging effect

The criteria used to compare the different tuning methods (ZN, SIMC, PSO, RECCO) of the control loop under the presence of slugging are:

- The evaluation of the overshoot percentage while rejecting the disturbance (in %)
- The evaluation of the time needed to eliminate the disturbance and reach the set point again (in seconds)

Table III.5 given above shows the results of the simulation under slug flow rejection test case. According to these results and those shown in Figure III.13, it can be easily observed that the slugging effect is less effectively attenuated by the PID-ZN and PID-SIMC tuning methods. This is due to the recorded peaks in the responses and the relatively long time taken to compensate for them. In comparison to this, the PID-PSO and the RECCo achieved better performance despite the maximum peak of (1-10)% recorded during the rejection of the disturbance by the water level control loop. However, the RECCo method eliminates the slugging effect in a relatively short time compared to the other three methods which is a very promising result.

III.7 Conclusion

This chapter addressed the problem of designing efficient control laws for the water level loop of the 10-V-255 three-phase separator under study. To this, we considered advanced and conventional control techniques and studied more precisely on the tuning of PID controllers relying on ZN, SIMC and PSO methods, and also on designing an evolving data cloud-based PID-like controller (RECCo) for the separator level loop.

The simulation results clearly demonstrate how performance of the level controlled loop was improved by using the intelligent tuning mechanisms, namely the PID-PSO and the RECCo. Indeed, reasonable level reference tracking results have been achieved under the these two

artificial intelligence based control schemes as can be noticed from the obtained time responses. Compensating for the effect of slug flow is the other important objective tackled in the present study. Slugging compensation scenario has also shown reasonable results under the PID-PSO and the RECCo controllers. It is worth noting that this performance of RECCo control has been obtained even though the evolving intelligent RECCo controller is model-free and therefore no modeling is required for control design. This feature of RECCo control is of utmost importance for real-time implementation.

Conclusion

This work presents a proposal about the reconfiguration of the current control of the three-phase separator 10-V-255 which is actually operating in the GS1 centre of the Gassi El Agreb oil complex. The objective is focused on implementing a control strategy that effectively controls the main variables of the separator, namely the water level but it can also be implemented for the oil level and the gas pressure. The expected control performance is expressed in terms of maintaining the set values within their admissible operating limits, and especially compensating for the slugging effect governing the turbulent flows of hydrocarbon mixtures.

The study begins with an initial phase of understanding the operation of the three-phase separator and its currently installed control configuration, followed by a physical modelling step using the actual process parameters and dimensions. The control strategies are established based on the calculated models. They are developed using recent methods for designing conventional PID controllers, incorporating mechanisms for tuning the control parameters and model-free tuning. These calculations have resulted in PID-ZN, PID-SIMC, PID-PSO and RECCo control configurations, which have been validated and compared through simulation on the water level control loop of the three-phase separator.

The obtained results clearly demonstrate the superiority of the RECCo strategy which is basically model-free and almost parameter-free in view of the good performance on the control loop of water level. The dynamics of these variables are well maintained within operational limits, with very well-damped transients. The slugging effect is effectively compensated for, despite the severe simulation conditions imposed. The PID-SIMC and PID-ZN controllers with fixed parameters also achieve acceptable performance following the recent tuning techniques we used in this study.

Finally, we can expect a promising application of the RECCo controller in industrial automation, because it looks able to achieve the flexibility in control design while maintaining a good performance, all of this without needing a model for the controlled plant. The implementation of the proposed control configuration on the DCS system would also be of great interest from an industrial standpoint.

ANNEX A Simulation block diagrams

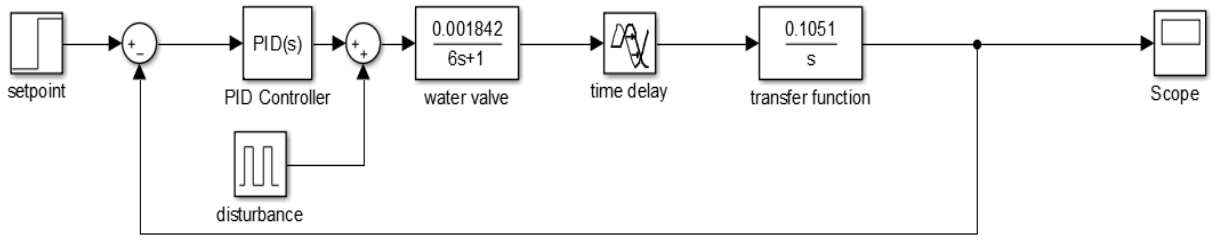

Figure A.1 Simulation model for the water level loop

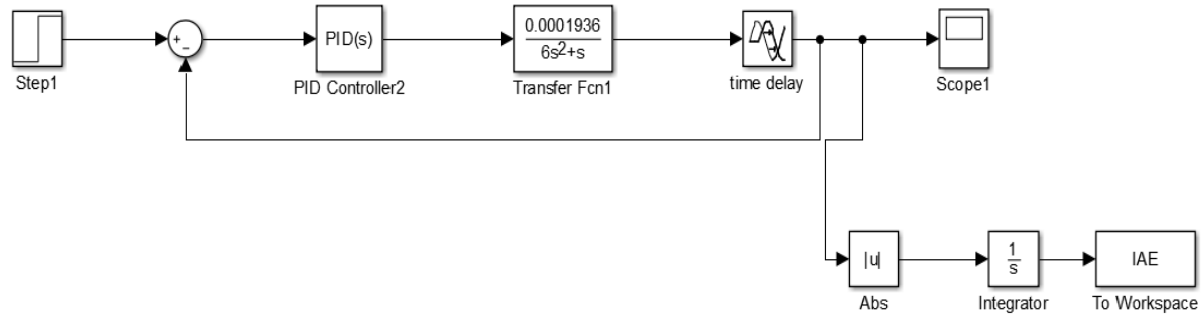

Figure A.2 Simulation model used for the particle swarm optimization method

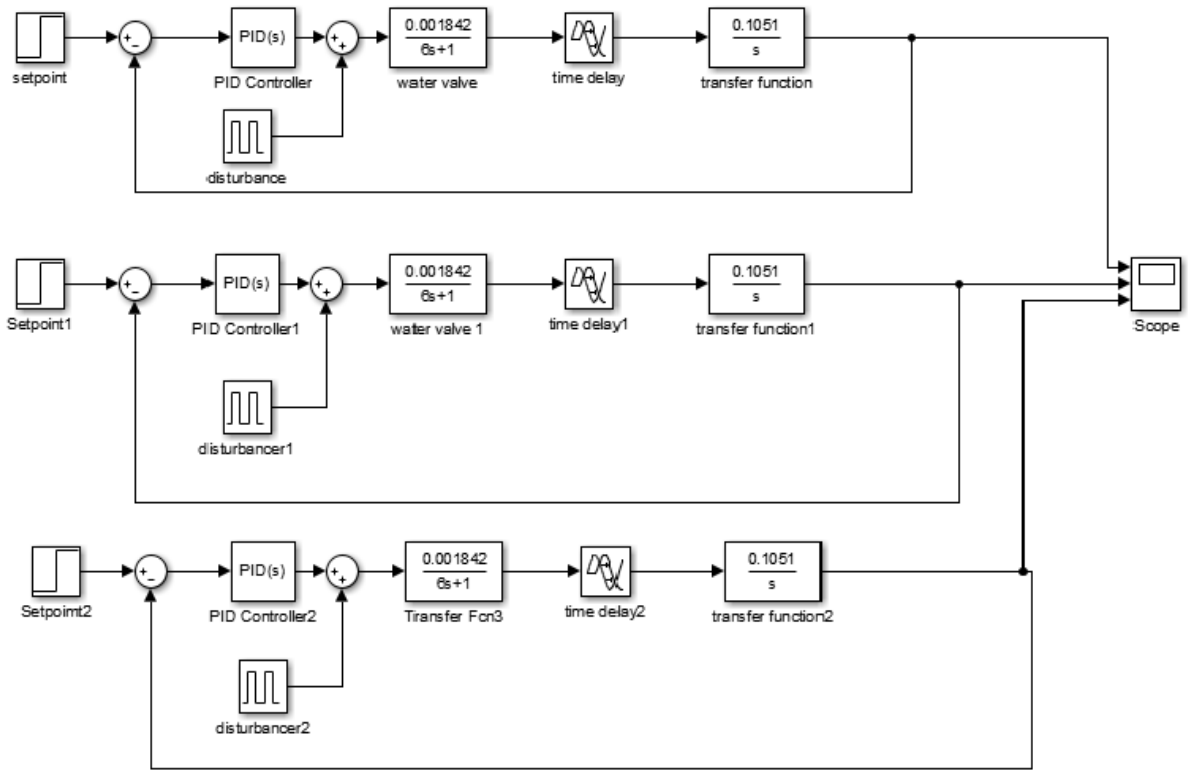

Figure A.3 PID-ZN, PID-SIMC, PID-PSO simulation models

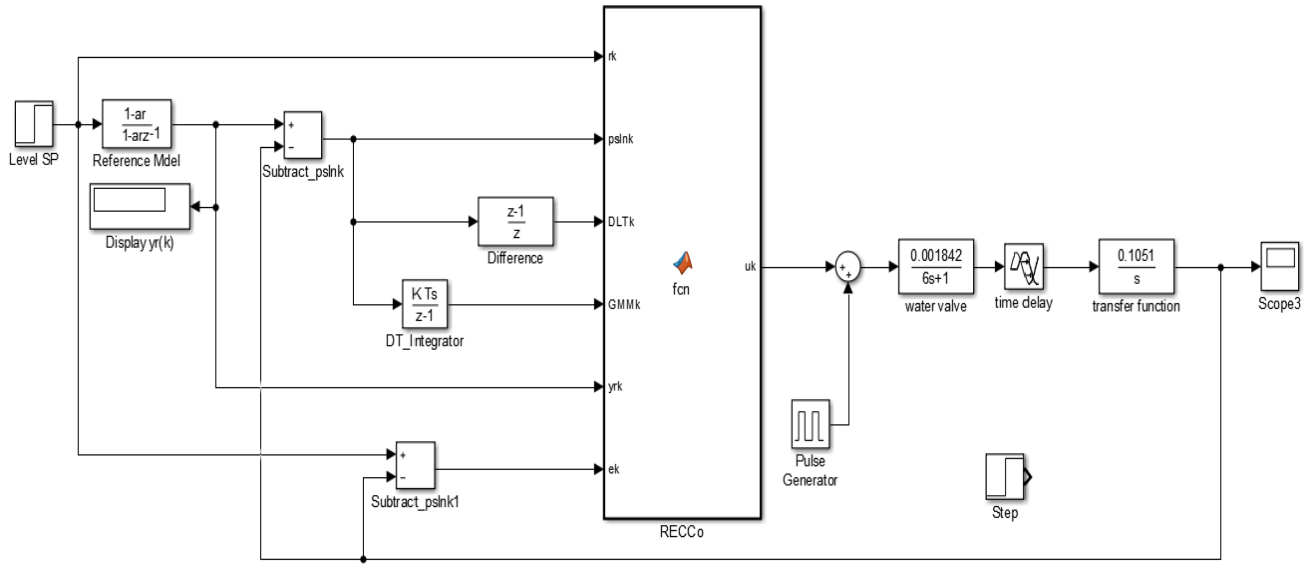

Figure A.4 RECCo simulation model

References

[1] Oil and gas separators - PetroWiki. https://petrowiki.spe.org/Oil_and_gas_separators

[2] Separator types - PetroWiki. https://petrowiki.spe.org/Separator_types

[3] Cyclone Inlet Device - Sulzer. https://www.sulzer.com/en/shared/products/cyclone-inlet-device

[4] Vane Pack - Sulzer. https://www.sulzer.com/en/shared/products/vane-pack

[5] Electrostatic Coalescers - Sulzer. https://www.sulzer.com/en/shared/products/electrostatic-coalescers

[6] Wire Mesh Pad - Sulzer. https://www.sulzer.com/en/shared/products/wire-mesh-pad

[7] Support de formation TOTAL: EXP-RP-EQ0800-FR, les équipements, les séparateurs, 2007

[8] S.Mokhatab, W.A.Poe, Handbook of natural Gas tansmission and processing , Senior gas processing/LNG consultant, Dartmouth, NS, Canada, Second Edition, 2012

[9] China Oil HBP Group, Dispositifs de soupape à voie multiple. From website: http://chine-hbp.com

[10] M. Wilhelmsen Control Structure and Tuning Method Design for suppressing Disturbances in a multi-phase Separator, Thesis of Norwegian University of Science and Technology, 2013

[11] Atalla F. Sayda and James H. Taylor Modeling and Control of Three-Phase Gravity Separators in Oil Production Facilities, 2007 American Control Conference, july 2007.

[12] CIRA instrumentation, Vannes de régulation, From website : http://cirainstrumentation.fr

[13] Skogestad, S. and Postlethwaite, I. (2005). Multivariable Feedback Control: Analysis and Design, 2nd Edition. John Wiley & Sons.

[14] P. Angelov, R. Yager, Simplified fuzzy rule-based systems using non-parametric antecedents and relative data density, in: 2011 IEEE Workshop on Evolving and Adaptive Intelligent Systems (EAIS), April, 2011, pp. 62–69.

[15] P. Angelov, I. Skrjanc, S. Blazic, Robust evolving cloud-based controller for a hydraulic plant, in: 2013 IEEE Conference on Evolving and Adaptive Intelligent Systems (EAIS), April, 2013, pp. 1–8.

[16] I. Skrjanc, S. Blazic, P. Angelov, Robust evolving cloud-based PID control adjusted by gradient learning method, in: 2014 IEEE Conference on Evolving and Adaptive Intelligent Systems (EAIS), June, 2014, pp. 1–8.

[17] Skogestad, S. and Postlethwaite, I. (2005). Multivariable Feedback Control: Analysis and Design, 2nd Edition. John Wiley & Sons.

[18] A.Khellassi, «Cours sur l'Automatisation des Systèmes Industriels», UMBB, Boumerdes, Novembre 2014

[19] S.Skogestad, Simple analytic rules for model reduction and PID controller tuning, Journal of Process Control, 2003

[20] Clerc, M. (2006). Particle Swarm Optimization (1st ed.). ISTE Ltd.